

1           **Geochemistry of the dissolved loads of rivers in Southeast Coastal Region,**  
2           **China: Anthropogenic impact on chemical weathering and carbon sequestration**

3           Wenjing Liu<sup>1,2,3,4</sup>, Zhifang Xu<sup>1,2,3,4\*</sup>, Huiguo Sun<sup>1,2,3,4</sup>, Tong Zhao<sup>1,2,3,4</sup>, Chao Shi<sup>1,4</sup>, Taoze Liu<sup>5</sup>

4           <sup>1</sup>Key Laboratory of Cenozoic Geology and Environment, Institute of Geology and Geophysics,  
5           Chinese Academy of Sciences, Beijing 100029, China

6           <sup>2</sup>CAS Center for Excellence in Life and Paleoenvironment, Beijing, 100044, China

7           <sup>3</sup>Institutions of Earth Science, Chinese Academy of Sciences, Beijing 100029, China

8           <sup>4</sup>University of Chinese Academy of Sciences, Beijing 100049, China

9           <sup>5</sup>State Key Laboratory of Environmental Geochemistry, Institute of Geochemistry, Chinese  
10          Academy of Sciences, Guiyang, Guizhou 550002, China

11          \* Corresponding author. zfxu@mail.iggcas.ac.cn (Zhifang Xu, Tel: +86 10 82998289)

12 **Abstract:**

13 Southeast coastal region is the most developed and populated area in China.  
14 Meanwhile, it has been the most severe acid rain impacted region for many years. The  
15 chemical compositions and carbon isotope ratio of dissolved inorganic carbon ( $\delta^{13}\text{C}_{\text{DIC}}$ )  
16 of rivers were investigated to evaluate the chemical weathering and associated  
17 atmospheric  $\text{CO}_2$  consumption rates. Mass balance calculation indicated that the  
18 dissolved loads of major rivers in the Southeast Coastal Rivers Basin (SECRB) were  
19 contributed by atmospheric (14.3%, 6.6-23.4%), anthropogenic (15.7%, 0-41.1%),  
20 silicate weathering (39.5%, 17.8-74.0%) and carbonate weathering inputs (30.6%, 3.9-  
21 62.0%). The silicate and carbonate chemical weathering rates for these river  
22 watersheds were  $14.2\text{-}35.8 \text{ t km}^{-2} \text{ a}^{-1}$  and  $1.8\text{-}52.1 \text{ t km}^{-2} \text{ a}^{-1}$ , respectively. The associated  
23 mean  $\text{CO}_2$  consumption rate by silicate weathering for the whole SECRB were  $218 \times 10^3$   
24  $\text{mol km}^{-2} \text{ a}^{-1}$ . The chemical and  $\delta^{13}\text{C}_{\text{DIC}}$  evidences indicated that sulfuric acid (mainly  
25 from acid deposition) was significantly involved in chemical weathering of rocks. The  
26 calculation showed an overestimation of  $\text{CO}_2$  consumption at  $0.14 \times 10^{12} \text{ g C a}^{-1}$  if  
27 sulfuric acid was ignored, which accounted for about 24% of the total  $\text{CO}_2$  consumption  
28 by silicate weathering in the SECRB. This study quantitatively highlights that the role  
29 of sulfuric acid in chemical weathering, suggesting that acid deposition should be  
30 considered in studies of chemical weathering and associated  $\text{CO}_2$  consumption.

31 **Keywords:** Southeast Coastal Rivers Basin; Chemical weathering;  $\text{CO}_2$  consumption;  
32 acid deposition;

33

## 34 **1. Introduction**

35       Chemical weathering of rocks is a key process that links geochemical cycling of  
36 solid earth to the atmosphere and ocean. It provides nutrients to terrestrial and marine  
37 ecosystems and regulates the level of atmospheric CO<sub>2</sub>. As a net sink of atmospheric  
38 CO<sub>2</sub> on geologic timescales, estimation of silicate chemical weathering rates and the  
39 controlling factors are important issues related to long-term global climate change (e.g.  
40 Raymo and Ruddiman, 1992; Négrel et al. 1993; Berner and Caldeira, 1997; Gaillardet  
41 et al., 1999; Kump et al., 2000; Amiotte-Suchet et al., 2003; Oliva et al., 2003;  
42 Hartmann et al., 2009; Moon et al., 2014). As an important component in the Earth's  
43 Critical Zone (U.S. Nat. Res. Council Comm., 2001), river serves as an integrator of  
44 various natural and anthropogenic processes and products in a basin, and a carrier  
45 transporting the weathering products from continent to ocean. Therefore, the chemical  
46 compositions of river are widely used to evaluate chemical weathering and associated  
47 CO<sub>2</sub> consumption rates at catchment and/or continental scale, and examine their  
48 controlling factors (e.g., Edmond et al., 1995; Gislason et al., 1996; Galy and France-  
49 Lanord, 1999; Huh, 2003; Millot et al., 2002, 2003; Oliva et al., 2003; West et al., 2005;  
50 Moon et al., 2007; Noh et al., 2009; Shin et al., 2011; Calmels et al., 2011; Li, S., et al.  
51 2014).

52       With the intensification of human activities, human perturbations to river basins  
53 have increased in frequency and magnitude (Raymond et al., 2008; Regnier et al., 2013;  
54 Li and Bush, 2015). It is important to understand how such perturbations function on  
55 the current weathering systems and to predict how they will affect the Critical Zone of

56 the future (Brantley and Lebedeva, 2011). In addition to CO<sub>2</sub>, other sources of acidity  
57 (such as sulfuric, nitric and organic acids) can also produce protons. These protons react  
58 with carbonate and silicate minerals, thus enhance rock chemical weathering rate and  
59 flux compared with only considering protons deriving from CO<sub>2</sub> dissolution (Calmels  
60 et al., 2007; Xu and Liu, 2010). The effect of other sourced proton (especially H<sup>+</sup>  
61 induced by SO<sub>2</sub> and NO<sub>x</sub> coming from anthropogenic activities) on chemical  
62 weathering is documented to be an important mechanism modifying atmospheric CO<sub>2</sub>  
63 consumption by rock weathering (Galy and France-Lanord, 1999; Semhi, et al., 2000;  
64 Spence and Telmer, 2005; Xu and Liu, 2007; Perrin et al., 2008; Gandois et al., 2011).  
65 Anthropogenic emissions of SO<sub>2</sub> was projected to provide 3 to 5 times greater H<sub>2</sub>SO<sub>4</sub>  
66 to the continental surface than the pyrite oxidation originated H<sub>2</sub>SO<sub>4</sub> (Lerman et al.,  
67 2007). Therefore, increasing acid precipitation due to intense human activities  
68 nowadays could make this mechanism more prominently.

69 The role of acid precipitation on the chemical weathering and CO<sub>2</sub> consumption  
70 has been investigated in some river catchments (Amiotte-Suchet et al., 1995; Probst et  
71 al., 2000; Vries et al., 2003; Lerman et al., 2007; Xu and Liu, 2010). It has been  
72 documented that silicate rocks were more easily disturbed by acid precipitation during  
73 their weathering and soil leaching processes, because of their low buffering capacity  
74 (Reuss et al., 1987; Amiotte-Suchet et al., 1995). The disturbance could be intensive  
75 and cause a decrease of CO<sub>2</sub> consumption about 73% by weathering due to acid  
76 precipitation in the Strengbach catchment (Vosges Mountains, France), where is  
77 dominated by crystalline rocks (Amiotte-Suchet et al., 1995). This highlights the

78 importance of exploring anthropogenic impact on chemical weathering and CO<sub>2</sub>  
79 consumption under different background (e.g. lithology, climate, human activity  
80 intensity, and basin scale) for better constraining and estimation of acid precipitation  
81 effect on rock weathering. Asia, especially East Asia, is one of the world's major sulfur  
82 emissions areas. However, the effect of acid precipitation on silicate weathering and  
83 associated CO<sub>2</sub> consumption was not well evaluated in this area, especially lack of  
84 quantitative studies.

85 Southeast coastal region of China is the most highly developed and populated area  
86 in China, dominated by Mesozoic magmatic rocks (mainly granite and volcanic rocks)  
87 in lithology. Meanwhile, it is also seriously impacted by acid rain, with a volume-  
88 weighted mean value of pH lower than 4.5 for many years (Wang et al., 2000; Larssen  
89 and Carmichael, 2000; Zhao, 2004; Han et al., 2006; Larssen et al., 2006; Zhang et al.,  
90 2007a; Huang et al., 2008; Xu et al., 2011). Therefore, it is an ideal area for evaluating  
91 silicate weathering and the effect of acid rain. In this study, the chemical and carbon  
92 isotope composition of rivers in this area were first systematically investigated, in order  
93 to: (i) decipher the different sources of solutes and to quantify their contributions to the  
94 dissolved loads; (ii) calculate silicate weathering and associated CO<sub>2</sub> consumption rates;  
95 (iii) evaluate the effects of acid deposition on rock weathering and CO<sub>2</sub> consumption  
96 flux.

## 97 **2. Natural setting of study area**

98 Southeast coastal region of China, where the landscape is dominated by  
99 mountainous and hilly terrain, and lacks the conditions for breeding large rivers. The

100 rivers in this region is dominantly small and medium-sized due to the topographic  
101 limitation. Only 5 rivers in this region have length over 200 km and the drainage area  
102 over 10,000 km<sup>2</sup>, and they are in turn from north to south: Qiantangjiang (Qiantang)  
103 and Oujiang (Ou) in Zhejiang province; Minjiang (Min) and Jiulongjiang (Jiulong) in  
104 Fujian province; Han Jiang (Han) in Guangdong province (Fig. 1). Rivers in this region  
105 generally flow eastward or southward and finally inject into the East China Sea or the  
106 South China Sea (Fig. 1), and they are collectively named as ‘Southeast Coastal Rivers’  
107 (SECRs).

108 The Southeast Coastal Rivers Basin (SECRB) belongs to the warm and humid  
109 subtropical oceanic monsoon climate. The average annual temperature and  
110 precipitation are 17-21°C and 1400-2000 mm, respectively. The precipitation mainly  
111 happens during May to September, and the minimum and maximum temperature often  
112 occurs in January and July. This area is one of the most developed areas in China, with  
113 a population more than 190 million (mean density of ~470 individuals/km<sup>2</sup>), but the  
114 population mainly concentrated in the coastal urban areas. The vegetation coverage of  
115 these river basins is more than 60%, mainly subtropical evergreen-deciduous broadleaf  
116 forest and mostly distributing in mountains area. Cultivated land, and industries and  
117 cities are mainly located in the plain areas and lower reach of these rivers.

118 Geologically, three regional-scale fault zones are distributed across the SECRB  
119 region (Fig. 1). They are the sub-EW-trending Shaoxing-Jiangshan fault zone, the NE-  
120 trending Zhenghe-Dapu fault zone, and the NE-trending Changle-Nanao fault zone  
121 (Shu et al., 2009). These fault zones dominate the direction of the mountains ridgelines

122 and drainages, as well as the formation of the basins and bay. The Zhenghe-Dapu fault  
123 zone is a boundary line of Caledonian uplift belt and Hercynian-Indosinian depression  
124 zone. Mesozoic magmatic rocks are widespread in the southeast coastal region with a  
125 total outcrop area at about 240,000 km<sup>2</sup>. Over 90% of the Mesozoic magmatic rocks  
126 are granitoids (granites and rhyolites) and their volcanic counterpart with minor  
127 existence of basalts (Zhou et al., 2000, 2006; Bai et al., 2014). These crust-derived  
128 granitic rocks are mainly formed in the Yanshanian stage, and may have been related to  
129 multiple collision events between Cathaysia and Yangtze blocks and Pacific plate (Zhou  
130 and Li, 2000; Xu et al., 2016). Among the major river basins, the proportions of  
131 magmatic rocks outcrop are about 36% in Qiantang river basin, above 80% in Ou,  
132 Jiaoxi and Jin river basins, and around 60% in Min, Jiulong, Han and Rong river basins  
133 (Shi, 2014). The overlying Quaternary sediment in this area is composed of brown-  
134 yellow siltstones but is rarely developed. The oldest basement complex is composed of  
135 metamorphic rocks of greenschist and amphibolite facies. Sedimentary rocks categories  
136 into two types, one is mainly composed by red clastic rocks which cover more than  
137 40,000 km<sup>2</sup> in the study area; the other occurs as interlayers within volcanic formations,  
138 including varicolored mudstones and sandstones. They are mainly distributed on the  
139 west of Zhenghe-Dapu fault zone (FJBGRM, 1985; ZJBGMR, 1989; Shu et al., 2009).

### 140 **3. Sampling and analytical method**

141 A total of 121 water samples were collected from mainstream and tributaries of  
142 the major rivers in the SECRB from July 8th to 31 of 2010 in the high-flow period  
143 (sample number and locations are shown in Fig. 1). 2-L water samples were collected

144 in the middle channel of the river from bridges or ferries, or directly from the center of  
145 some shallow streams in the source area. The lower reaches sampling sites were  
146 selected distant away from the estuary to avoid the influence of seawater. Temperature  
147 (T), pH and electrical conductivity (EC) were measured in the field with a portable  
148 EC/pH meter (YSI-6920, USA). All of the water samples for chemical analysis were  
149 filtered in field through 0.22  $\mu\text{m}$  Millipore membrane filter, and the first portion of the  
150 filtration was discarded to wash the membrane and filter. One portion filtrate were  
151 stored directly in HDPE bottles for anion analysis and another were acidified to  $\text{pH} < 2$   
152 with 6 M double sub-boiling distilled  $\text{HNO}_3$  for cation analysis. All containers were  
153 previously washed with high-purity  $\text{HCl}$  and rinsed with Milli-Q 18.2  $\text{M}\Omega$  water.

154  $\text{HCO}_3^-$  was titrated with 0.005M  $\text{HCl}$  within 12 h after sampling. Cations ( $\text{Na}^+$ ,  $\text{K}^+$ ,  
155  $\text{Ca}^{2+}$  and  $\text{Mg}^{2+}$ ) were determined using Inductively Coupled Plasma Atomic Emission  
156 Spectrometer (ICP-AES) (IRIS Intrepid II XSP, USA). Anions ( $\text{Cl}^-$ ,  $\text{F}^-$ ,  $\text{NO}_3^-$  and  $\text{SO}_4^{2-}$ )  
157 were analyzed by ionic chromatography (IC) (Dionex Corporation, USA). Dissolved  
158 silica was determined by spectrophotometry using the molybdate blue method. Reagent  
159 and procedural blanks were measured in parallel to the sample treatment, and  
160 calibration curve was evaluated by quality control standards before, during and after  
161 the analyses of each batch of samples. Measurement reproducibility was determined by  
162 duplicated sample and standards, which showed  $\pm 3\%$  precision for the cations and  $\pm 5\%$   
163 for the anions.

164 River water samples for carbon isotopic ratio ( $\delta^{13}\text{C}$ ) of dissolved inorganic carbon  
165 (DIC) measurements were collected in 150 ml glass bottles with air-tight caps and

166 preserved with HgCl<sub>2</sub> to prevent biological activity. The samples were kept refrigerated  
167 until analysis. For the δ<sup>13</sup>C measurements, the filtered samples were injected into glass  
168 bottles with phosphoric acid. The CO<sub>2</sub> was then extracted and cryogenically purified  
169 using a high vacuum line. δ<sup>13</sup>C isotopic ratios were analyzed on Finnigen MAT-252  
170 stable isotope mass spectrometer at the State Key Laboratory of Environmental  
171 Geochemistry, Chinese Academy of Sciences. The results are expressed with reference  
172 to VPDB, as follows:

$$173 \quad \delta^{13}\text{C} = [((^{13}\text{C}/^{12}\text{C})_{\text{sample}} / (^{13}\text{C}/^{12}\text{C})_{\text{standard}}) - 1] \times 1000 \quad (1)$$

174 The δ<sup>13</sup>C measurement has an overall precision of 0.1‰. A number of duplicate  
175 samples were measured and the results show that the differences were less than the  
176 range of measurement accuracy.

#### 177 **4. Results**

178 The major parameter and ion concentrations of samples are given in Table 1. The  
179 pH values of water samples ranged from 6.50 to 8.24, with an average of 7.23. Total  
180 dissolved solids (TDS) of water samples varied from 35.3 to 205 mg l<sup>-1</sup>, with an average  
181 of 75.2 mg l<sup>-1</sup>. Compared with the major rivers in China, the average TDS was  
182 significantly lower than the Changjiang (224 mg l<sup>-1</sup>, Chetelat et al., 2008), the Huanghe  
183 (557 mg l<sup>-1</sup>, Fan et al., 2014) and the Zhujiang (190 mg l<sup>-1</sup>, Zhang et al., 2007b).  
184 However, the average TDS was comparable to the rivers draining silicate rock  
185 dominated areas, e.g. the upper Ganjiang in Ganzhou, south China (63 mg l<sup>-1</sup>, Ji and  
186 Jiang, 2012), the Amur in north China (70 mg l<sup>-1</sup>, Moon et al., 2009), the Xishui in  
187 Hubei, central China (101 mg l<sup>-1</sup>, Wu et al., 2013), and north Han river in South Korea

188 (75.5 mg l<sup>-1</sup>, Ryu et al., 2008). Among the major rivers in the SECRB, the Qiantang had  
189 the highest TDS value (averaging at 121 mg l<sup>-1</sup>), and the Ou had the lowest TDS value  
190 (averaging at 48.8 mg l<sup>-1</sup>).

191 Major ion compositions are shown in the cation and anion ternary diagrams (Fig.  
192 2a and b). In comparison with rivers (e.g. the Wujiang and Xijiang) draining carbonate  
193 rocks dominated area (Han and Liu, 2004; Xu and Liu, 2010), these rivers in the SECRB  
194 have distinctly higher proportions of Na<sup>+</sup>, K<sup>+</sup>, and dissolved SiO<sub>2</sub>. As shown in the Fig.  
195 2, most samples have high Na<sup>+</sup> and K<sup>+</sup> proportions, with an average more than 50% (in  
196 μmol l<sup>-1</sup>) of the total cations, except for samples from the Qiantang. The concentrations  
197 of Na<sup>+</sup> and K<sup>+</sup> range from 43.5 to 555 μmol l<sup>-1</sup> and 42.9 to 233 μmol l<sup>-1</sup>, with average  
198 values of 152 and 98 μmol l<sup>-1</sup>, respectively. The concentrations of dissolved SiO<sub>2</sub> range  
199 from 98.5 to 370 μmol l<sup>-1</sup>, with an average of 212 μmol l<sup>-1</sup>. Ca<sup>2+</sup> and Mg<sup>2+</sup> account for  
200 about 38% and 11.6% of the total cation concentrations. HCO<sub>3</sub><sup>-</sup> is the dominant anion  
201 with concentrations ranging from 139 to 1822 μmol l<sup>-1</sup>. On average, it comprises 60.6%  
202 (36-84.6%) of total anions on a molar basis, followed by SO<sub>4</sub><sup>2-</sup> (14.6%), Cl<sup>-</sup> (13.1%)  
203 and NO<sub>3</sub><sup>-</sup> (11.8%). The major ionic compositions indicate that water chemistry of these  
204 rivers in the SECRB is controlled by silicate weathering. Meanwhile, it is also  
205 influenced by carbonate weathering, especially in the Qiantang river system.

206 The δ<sup>13</sup>C of dissolved inorganic carbon in the rivers of the SECRB are given in  
207 Table 1. The δ<sup>13</sup>C of the water samples show a wide range, from -11.0‰ to -24.3‰  
208 (average -19.4‰), and with majority falling between -15 and -23‰. The values are  
209 similar to rivers draining Deccan Traps (Das et al., 2005).

## 210 **5. Discussion**

211 The dissolved solids in river water are commonly from atmospheric and  
212 anthropogenic inputs and weathering of rocks within the drainage basin. It is necessary  
213 to quantify the contribution of different sources to the dissolved loads before deriving  
214 chemical weathering rates and associated CO<sub>2</sub> consumption.

### 215 *5.1 Atmospheric and anthropogenic inputs*

216 To evaluate atmospheric inputs to river waters, chloride is the most common used  
217 reference. Generally, water samples that have the lowest Cl<sup>-</sup> concentrations are  
218 employed to correct the proportion of atmospheric inputs in a river system (Négrel et  
219 al., 1993; Gaillardet et al., 1997; Viers et al., 2001; Xu and Liu, 2007). In pristine areas,  
220 the concentration of Cl<sup>-</sup> in river water is assumed to be entirely derived from the  
221 atmosphere, provided that the contribution of evaporites is negligible (e.g. Stallard and  
222 Edmond, 1981; Négrel et al., 1993). In the SECRB, the lowest Cl<sup>-</sup> concentration was  
223 mainly found in the headwater of each river. According to the geologic setting, no salt-  
224 bearing rocks was found in these headwater area (FJBGRM, 1985; ZJBGMR, 1989). In  
225 addition, these areas are mainly mountainous and sparsely populated. Therefore, we  
226 assumed that the lowest Cl<sup>-</sup> concentration of samples from the headwater of each major  
227 river came entirely from atmosphere.

228 The proportion of atmosphere-derived ions in the river waters can then be  
229 calculated by using the element/Cl ratios of the rain. Chemical compositions of rain in  
230 the studied area have been reported at different sites, including Hangzhou, Jinhua,  
231 Nanping, Fuzhou and Xiamen (Zhao, 2004; Zhang et al., 2007a; Huang et al., 2008;

232 Cheng et al., 2011; Xu et al., 2011) (Fig. 1). The volume-weighted mean concentration  
233 of ions and Cl-normalized molar ratios are compiled in Table 2. According to this  
234 procedure, 6.6-23.4% (averaging 14.3%) of total dissolved cations in the major rivers  
235 of the SECRB originated from rain. Among the anions,  $\text{SO}_4^{2-}$  and  $\text{NO}_3^-$  in the rivers are  
236 mainly from the atmospheric input, averaging at 74.7% for  $\text{SO}_4^{2-}$  and 68.6% for  $\text{NO}_3^-$ ,  
237 respectively.

238 As the most developed and populated areas in China, the chemistry of rivers in the  
239 SECRB could be significantly impacted by anthropogenic inputs.  $\text{Cl}^-$ ,  $\text{NO}_3^-$  and  $\text{SO}_4^{2-}$   
240 are commonly associated with anthropogenic sources and have been used as tracers of  
241 anthropogenic inputs in watershed. High concentrations of  $\text{Cl}^-$ ,  $\text{NO}_3^-$  and  $\text{SO}_4^{2-}$  can be  
242 found at the lower reaches of rivers in the SECRB, and an obvious increase after  
243 flowing through plain areas and cities. This tendency indicates that river water  
244 chemistry is affected by anthropogenic inputs while passing through the catchments.  
245 After correcting for the atmospheric contribution to river waters, the following  
246 assumption is needed to quantitatively estimate the contributions of anthropogenic  
247 inputs. That is,  $\text{Cl}^-$  originates from only atmospheric and anthropogenic inputs, the  
248 excess of atmospheric  $\text{Cl}^-$  is regarded to present anthropogenic inputs and balanced by  
249  $\text{Na}^+$ .

## 250 *5.2 Chemical weathering inputs*

251 Water samples were displayed on a plot of Na-normalized molar ratios (Fig. 3).  
252 The values of the world's large rivers (Gaillardet et al. 1999) are also shown in the  
253 figure. A best correlations between elemental ratios were observed for  $\text{Ca}^{2+}/\text{Na}^+$  vs.

254  $\text{Mg}^{2+}/\text{Na}^+$  ( $R^2 = 0.95$ ,  $n = 120$ ) and  $\text{Ca}^{2+}/\text{Na}^+$  vs.  $\text{HCO}_3^-/\text{Na}^+$  ( $R^2 = 0.98$ ,  $n = 120$ ). The  
255 samples cluster on a mixing line mainly between silicate and carbonate end-members,  
256 closer to the silicate end-member, and with little evaporite contribution. This  
257 corresponds with the distribution of rock types in the SECRB. In addition, all water  
258 samples have equivalent ratios of  $(\text{Na}^+ + \text{K}^+)/\text{Cl}^-$  larger than one, indicating silicate  
259 weathering as the source of  $\text{Na}^+$  and  $\text{K}^+$  rather than chloride evaporites dissolution.

260 The geochemical characteristics of the silicate and carbonate end-members can be  
261 deduced from the correlations between elemental ratios and referred to literature data  
262 for catchments with well-constrained lithology. After correction for atmospheric inputs,  
263 the  $\text{Ca}^{2+}/\text{Na}^+$ ,  $\text{Mg}^{2+}/\text{Na}^+$  and  $\text{HCO}_3^-/\text{Na}^+$  of the river samples ranged from 0.31 to 30,  
264 0.16 to 6.7, and 1.1 to 64.2, respectively. According to the geological setting (Fig. 1),  
265 there are some small rivers draining purely silicate areas in the SECRs drainage basins.  
266 Based on the elemental ratios of these rivers, we assigned the silicate end-member for  
267 this study as  $\text{Ca}^{2+}/\text{Na}^+ = 0.41 \pm 0.10$ ,  $\text{Mg}^{2+}/\text{Na}^+ = 0.20 \pm 0.03$  and  $\text{HCO}_3^-/\text{Na}^+ = 1.7 \pm 0.6$ . The  
268 ratio of  $(\text{Ca}^{2+} + \text{Mg}^{2+})/\text{Na}^+$  for silicate end-member was 0.61, which is close to the  
269 silicate end-member of world rivers ( $(\text{Ca}^{2+} + \text{Mg}^{2+})/\text{Na}^+ = 0.59 \pm 0.17$ , Gaillardet et al.,  
270 1999). Moreover, several previous researches have documented the chemical  
271 composition of rivers, such as the Amur and the Songhuajiang in North China, the  
272 Xishui in the lower reaches of the Changjiang, and major rivers in South Korea (Moon  
273 et al., 2009; Liu et al., 2013; Wu et al., 2013; Ryu et al., 2008; Shin et al., 2011). These  
274 river basins has similar lithological setting with the study area, we could further validate  
275 the composition of silicate end-member with their results.  $\text{Ca}^{2+}/\text{Na}^+$  and  $\text{Mg}^{2+}/\text{Na}^+$

276 ratios of silicate end-member were reported for the Amur (0.36 and 0.22), the  
277 Songhuajiang (0.44±0.23 and 0.16), the Xishui (0.6±0.4 and 0.32±0.18), the Han (0.55  
278 and 0.21) and six major rivers in South Korea (0.48 and 0.20) in the studies above, well  
279 bracketing our estimation for silicate end-member.

280 Whereas, some samples show high concentrations of  $\text{Ca}^{2+}$ ,  $\text{Mg}^{2+}$  and  $\text{HCO}_3^-$ ,  
281 indicating the contribution of carbonate weathering. The samples collected in the upper  
282 reaches (Sample 12 and 13) in the Qiantang fall close to the carbonate end-member  
283 documented for world large rivers (Gaillardet et al., 1999). In the present study,  
284  $\text{Ca}^{2+}/\text{Na}^+$  ratio of 0.41±0.10 and  $\text{Mg}^{2+}/\text{Na}^+$  ratio of 0.20±0.03 for silicate end-member  
285 are used to calculate the contribution of  $\text{Ca}^{2+}$  and  $\text{Mg}^{2+}$  from silicate weathering. Finally,  
286 residual  $\text{Ca}^{2+}$  and  $\text{Mg}^{2+}$  are apportioned to carbonate weathering.

### 287 *5.3 Chemical weathering rate in the SECRBs*

288 Based on the above assumption, a forward model is employed to quantify the  
289 relative contribution of the different sources to the rivers of the SECRB in this study.  
290 (e.g. Galy and France-Lanord, 1999; Moon et al., 2007; Xu and Liu, 2007; 2010; Liu  
291 et al., 2013). The calculated contributions of different reservoir to the total cationic  
292 loads for large rivers and their major tributaries in the SECRB are presented in Fig. 4.  
293 On average, the dissolved cationic loads of the rivers in the study area originate  
294 dominantly from silicate weathering, which accounts for 39.5% (17.8-74.0%) of the  
295 total cationic loads in molar unit. Carbonate weathering and anthropogenic inputs  
296 account for 30.6% (3.9-62.0%) and 15.7% (0-41.1%), respectively. Contributions from  
297 silicate weathering are high in the Ou (55.6%), the Huotong (54.5%), the Ao (48.3%)

298 and the Min (48.3%) river catchments, which dominated by granitic and volcanic  
299 bedrocks. In contrast, high contribution from carbonate weathering is observed in the  
300 Qiantang (54.0%), the Jin (52.2%) and the Jiulong (44.8%) river catchments. The  
301 results manifest the lithology control on river solutes of drainage basin.

302 The chemical weathering rate of rocks is estimated by the mass budget, basin area  
303 and annual discharge (data from the Annual Hydrological Report P. R. China, 2010,  
304 Table 3), expressed in  $\text{ton km}^{-2} \text{ a}^{-1}$ . The silicate weathering rate (SWR) is calculated  
305 using major cationic concentrations from silicate weathering and assuming that all  
306 dissolved  $\text{SiO}_2$  is derived from silicate weathering (Xu and Liu, 2010), as the equation  
307 below:

$$308 \quad \text{SWR} = ([\text{Na}]_{\text{sil}} + [\text{K}]_{\text{sil}} + [\text{Ca}]_{\text{sil}} + [\text{Mg}]_{\text{sil}} + [\text{SiO}_2]_{\text{riv}}) \times \text{discharge} / \text{area} \quad (2)$$

309 The assumption about Si could lead to overestimation of the silicate weathering  
310 rate, as part of silica may come from dissolution of biogenic sources rather than the  
311 weathering of silicate minerals (Millet et al., 2003; Shin et al., 2011). Thus, the cationic  
312 silicate weathering rates ( $\text{Cat}_{\text{sil}}$ ) were also calculated.

313 The carbonate weathering rate (CWR) is calculated based on the sum of  $\text{Ca}^{2+}$ ,  
314  $\text{Mg}^{2+}$  and  $\text{HCO}_3^-$  from carbonate weathering, with half of the  $\text{HCO}_3^-$  coming from  
315 carbonate weathering being derived from the atmosphere  $\text{CO}_2$ , as the equation below:

$$316 \quad \text{CWR} = ([\text{Ca}]_{\text{carb}} + [\text{Mg}]_{\text{carb}} + 1/2[\text{HCO}_3]_{\text{carb}}) \times \text{discharge} / \text{area} \quad (3)$$

317 The chemical weathering rate and flux are calculated for major rivers and their  
318 main tributaries in the SECRB, and the results are shown in Table 3. Silicate and  
319 carbonate weathering fluxes of these rivers (SWF and CWF) range from  $0.02 \times 10^6 \text{ t a}^{-1}$

320 <sup>1</sup> to  $1.80 \times 10^6 \text{ t a}^{-1}$ , and from  $0.004 \times 10^6 \text{ t a}^{-1}$  to  $1.74 \times 10^6 \text{ t a}^{-1}$ , respectively. Among the  
321 rivers, the Min has the highest silicate weathering flux, and the Qiantang has the highest  
322 carbonate weathering flux. On the whole SECRB scale,  $3.95 \times 10^6 \text{ t a}^{-1}$  and  $4.09 \times 10^6 \text{ t}$   
323  $\text{a}^{-1}$  of dissolved solids originating from silicate and carbonate weathering, respectively,  
324 are transported into the East and South China Sea by rivers in this region. Compared  
325 with the largest three river basins (the Changjiang, the Huanghe and the Xijiang) in  
326 China, the flux of silicate weathering calculated for the SECRB is lower than the  
327 Changjiang ( $9.5 \times 10^6 \text{ t a}^{-1}$ , Gaillardet et al. 1999), but higher than the Huanghe  
328 ( $1.52 \times 10^6 \text{ t a}^{-1}$ , Fan et al., 2014) and the Xijiang ( $2.62 \times 10^6 \text{ t a}^{-1}$ , Xu and Liu, 2010).

329 The silicate and carbonate chemical weathering rates for these river watersheds  
330 were  $14.2\text{-}35.8 \text{ t km}^{-2} \text{ a}^{-1}$  and  $1.8\text{-}52.1 \text{ t km}^{-2} \text{ a}^{-1}$ , respectively. The total rock weathering  
331 rate (TWR) for the whole SECRB is  $48.1 \text{ ton km}^{-2} \text{ a}^{-1}$ , higher than the world average  
332 ( $24 \text{ ton km}^{-2} \text{ a}^{-1}$ , Gaillardet et al., 1999). The cationic silicate weathering rates ( $\text{Cat}_{\text{sil}}$ )  
333 ranges from  $4.7$  to  $12.0 \text{ ton km}^{-2} \text{ a}^{-1}$  for the river watersheds in the SECRB, averaging  
334 at  $7.8 \text{ ton km}^{-2} \text{ a}^{-1}$ . Furthermore, a good linear correlation ( $R^2 = 0.77$ ,  $n = 28$ ) is observed  
335 between the  $\text{Cat}_{\text{sil}}$  and runoff (Fig. 5), indicating silicate weathering rates is controlled  
336 by the runoff as documented in previous researches (e.g., Bluth and Kump, 1994;  
337 Gaillardet et al., 1999; Millot et al., 2002; Oliva et al., 2003; Wu et al., 2013; Pepin et  
338 al., 2013).

#### 339 *5.4 CO<sub>2</sub> consumption and the role of sulfuric acid*

340 To calculate atmospheric CO<sub>2</sub> consumption by silicate weathering (CSW) and by  
341 carbonate weathering (CCW), a charge-balanced state between rock chemical

342 weathering-derived alkalinity and cations was assumed (Roy et al., 1999).

$$343 \quad [\text{CO}_2]_{\text{CSW}} = [\text{HCO}_3]_{\text{CSW}} = [\text{Na}]_{\text{sil}} + [\text{K}]_{\text{sil}} + 2[\text{Ca}]_{\text{sil}} + 2[\text{Mg}]_{\text{sil}} \quad (4)$$

$$344 \quad [\text{CO}_2]_{\text{CCW}} = [\text{HCO}_3]_{\text{CCW}} = [\text{Ca}]_{\text{carb}} + [\text{Mg}]_{\text{carb}} \quad (5)$$

345 The calculated CO<sub>2</sub> consumption rates by chemical weathering for the studied  
346 rivers in SECRB are shown in Table 3. CO<sub>2</sub> consumption rates by carbonate and silicate  
347 weathering are from 17.9 to 530×10<sup>3</sup> mol km<sup>-2</sup> a<sup>-1</sup> (averaging at 206×10<sup>3</sup> mol km<sup>-2</sup> a<sup>-1</sup>)  
348 and from 167 to 460×10<sup>3</sup> mol km<sup>-2</sup> a<sup>-1</sup> (averaging at 281×10<sup>3</sup> mol km<sup>-2</sup> a<sup>-1</sup>) for major  
349 river catchments in the SECRB. The CO<sub>2</sub> consumption rates by silicate weathering in  
350 the SECRB are higher than that of major rivers in the world and China, such as the  
351 Amazon (174×10<sup>3</sup> mol km<sup>-2</sup> a<sup>-1</sup>, Mortatti and Probst, 2003), the Mississippi and the  
352 Mackenzie (66.8 and 34.1×10<sup>3</sup> mol km<sup>-2</sup> a<sup>-1</sup>, Gaillardet et al., 1999), the Changjiang  
353 (112×10<sup>3</sup> mol km<sup>-2</sup> a<sup>-1</sup>, Chetelat et al., 2008), the Huanghe (35×10<sup>3</sup> mol km<sup>-2</sup> a<sup>-1</sup>, Fan et  
354 al., 2014), the Xijiang (154×10<sup>3</sup> mol km<sup>-2</sup> a<sup>-1</sup>, Xu and Liu, 2010), the Longchuanjiang  
355 (173×10<sup>3</sup> mol km<sup>-2</sup> a<sup>-1</sup>, Li et al., 2011) and the Mekong (191×10<sup>3</sup> mol km<sup>-2</sup> a<sup>-1</sup>, Li et al.,  
356 2014) and three large rivers in eastern Tibet (103-121×10<sup>3</sup> mol km<sup>-2</sup> a<sup>-1</sup>, Noh et al.,  
357 2009), the Hanjiang in central China (120×10<sup>3</sup> mol km<sup>-2</sup> a<sup>-1</sup>, Li et al., 2009) and the  
358 Sonhuajiang in north China (66.6×10<sup>3</sup> mol km<sup>-2</sup> a<sup>-1</sup>, Liu et al., 2013). The high CO<sub>2</sub>  
359 consumption rates by silicate weathering in the SECRB could be attributed to extensive  
360 distribution of silicate rocks, high runoff, humid and hot climatic conditions. The  
361 regional fluxes of CO<sub>2</sub> consumption by silicate and carbonate weathering is about  
362 47.9×10<sup>9</sup> mol a<sup>-1</sup> (0.57×10<sup>12</sup> g C a<sup>-1</sup>) and 41.9×10<sup>9</sup> mol a<sup>-1</sup> (0.50×10<sup>12</sup> g C a<sup>-1</sup>) in the  
363 SECRB.

364           However, in addition to CO<sub>2</sub>, H<sub>2</sub>SO<sub>4</sub> is well documented as a significant proton  
365 provider in rock weathering process (Galy and France-Lanord, 1999; Karim and Veizer,  
366 2000; Yoshimura et al., 2001; Han and Liu, 2004; Spence and Telmer, 2005; Lerman  
367 and Wu, 2006; Xu and Liu 2007; 2010). Sulfuric acid can be generated by natural  
368 oxidation of pyrite and anthropogenic emissions of SO<sub>2</sub> from coal combustion and  
369 subsequently dissolve carbonate and silicate minerals. The consumption of CO<sub>2</sub> by rock  
370 weathering would be overestimated if H<sub>2</sub>SO<sub>4</sub> induced rock weathering is ignored  
371 (Spence and Telmer, 2005; Xu and Liu, 2010; Shin et al., 2011). Thus, the role of  
372 sulfuric acid on the chemical weathering is crucial for an accurate estimation of CO<sub>2</sub>  
373 consumption by rock weathering.

374           Rapid economic growth and increased energy demand have result in severe air  
375 pollution problems in China, indicated by the high levels of mineral acids  
376 (predominately sulfuric) observed in precipitation (Lassen and Carmichael, 2000; Pan  
377 et al., 2013; Liu et al., 2016). The national SO<sub>2</sub> emissions in 2010 reached to 30.8  
378 Tg/year (Lu et al., 2011). Previous study documented that fossil fuel combustion  
379 accounts for the dominant sulfur deposition (~77%) in China (Liu et al., 2016).  
380 Southeast coastal region is the most severe acid rain polluted region in China, with a  
381 volume-weighted mean value of pH lower than 4.5 for many years (Wang et al., 2000;  
382 Larssen and Carmichael, 2000; Zhao, 2004; Larssen et al., 2006). Current sulfur and  
383 nitrogen depositions in the Southeast coastal region are still among the highest in China  
384 (Fang et al., 2013; Cui et al., 2014; Liu et al., 2016).

385           The involvement of protons originating from H<sub>2</sub>SO<sub>4</sub> in the river waters can be

386 verified by the stoichiometry between cations and anions, shown in Fig. 6. In the rivers  
387 of the SECRB, the sum cations released by silicate and carbonate weathering were not  
388 balanced by either  $\text{HCO}_3^-$  or  $\text{SO}_4^{2-}$  (Fig. 6a), but were almost balanced by the sum of  
389  $\text{HCO}_3^-$  and  $\text{SO}_4^{2-}$  (Fig. 6b). This implies that both  $\text{H}_2\text{CO}_3$  and  $\text{H}_2\text{SO}_4$  are the potential  
390 erosion agents in chemical weathering in the SECRB. The  $\delta^{13}\text{C}$  values of the water  
391 samples show a wide range, from -11.0‰ to -24.3‰, with an average of -19.4‰. The  
392  $\delta^{13}\text{C}$  from soil is governed by the relative contribution from  $\text{C}_3$  and  $\text{C}_4$  plant (Das et al.,  
393 2005). The studied areas have subtropical temperatures and humidity, and thus  $\text{C}_3$   
394 processes are dominant. The  $\delta^{13}\text{C}$  of soil  $\text{CO}_2$  is derived primarily from  $\delta^{13}\text{C}$  of organic  
395 material which typically has a value of -24 to -34‰, with an average of -28‰ (Faure,  
396 1986). According to previous studies, the average value for  $\text{C}_3$  trees and shrubs are from  
397 -24.4 to -30.5‰, and most of them are lower than -28‰ in south China (Chen et al.,  
398 2005; Xiang, 2006; Dou et al., 2013). After accounting for the isotopic effect from  
399 diffusion of  $\text{CO}_2$  from soil, the resulting  $\delta^{13}\text{C}$  (from the terrestrial  $\text{C}_3$  plant process)  
400 should be  $\sim$  -25‰ (Cerling et al., 1991). This mean DIC derived from silicate  
401 weathering by carbonic acid (100% from soil  $\text{CO}_2$ ) would yield a  $\delta^{13}\text{C}$  value of -25‰.  
402 Carbonate rocks are generally derived from marine system and, typically, have  $\delta^{13}\text{C}$   
403 value close to zero (Das et al., 2005). Thus, the theoretical  $\delta^{13}\text{C}$  value of DIC derived  
404 from carbonate weathering by carbonic acid (50% from soil  $\text{CO}_2$  and 50% from  
405 carbonate rocks) is -12.5‰. DIC derived from carbonate weathering by sulfuric acid  
406 are all from carbonate rocks, thus the  $\delta^{13}\text{C}$  of the DIC would be 0‰. Based on these  
407 conclusions, sources of riverine DIC from different end-members in the SECRB were

408 plotted in Fig. 7. Most water samples drift away from the three endmember mixing area  
409 (carbonate and silicate weathering by carbonic acid and carbonate weathering by  
410 sulfuric acid) and towards the silicate weathering by H<sub>2</sub>SO<sub>4</sub> area, clearly illustrating the  
411 effect of sulfuric acid on silicate weathering.

412 Considering the H<sub>2</sub>SO<sub>4</sub> effect on chemical weathering, CO<sub>2</sub> consumption by  
413 silicate weathering can be determined from the equation below (Moon et al., 2007;  
414 Ryu et al., 2008; Shin et al., 2011):

$$415 \quad [\text{CO}_2]_{\text{SSW}} = [\text{Na}]_{\text{sil}} + [\text{K}]_{\text{sil}} + 2[\text{Ca}]_{\text{sil}} + 2[\text{Mg}]_{\text{sil}} - \gamma \times 2[\text{SO}_4]_{\text{atmos}} \quad (6)$$

416 Where  $\gamma$  is calculated by  $\text{cation}_{\text{sil}} / (\text{cation}_{\text{sil}} + \text{cation}_{\text{carb}})$ .

417 Based on the calculation in section 5.1, SO<sub>4</sub><sup>2-</sup> in river waters were mainly derived  
418 from atmospheric input. Assuming sulfate in rivers derived from atmospheric input  
419 (after correction for sea-salt contribution) are all from acid precipitation, CO<sub>2</sub>  
420 consumption rates by silicate weathering (SSW) are estimated between  $93 \times 10^3 \text{ mol km}^{-2}$   
421  $\text{a}^{-1}$  and  $336 \times 10^3 \text{ mol km}^{-2} \text{ a}^{-1}$  for major river watersheds in the SECRB. For the whole  
422 SECRB, the actual CO<sub>2</sub> consumption rates by silicate is  $218 \times 10^3 \text{ mol km}^{-2} \text{ a}^{-1}$  when the  
423 effect of H<sub>2</sub>SO<sub>4</sub> is considered. The flux of CO<sub>2</sub> consumption is overestimated by  
424  $11.5 \times 10^9 \text{ mol a}^{-1}$  ( $0.14 \times 10^{12} \text{ g C a}^{-1}$ ) due to the involvement of sulfuric acid from acid  
425 precipitation, accounting for approximately 23.9% of total CO<sub>2</sub> consumption flux by  
426 silicate weathering in the SECRB. It highlights the fact that the drawdown of  
427 atmospheric CO<sub>2</sub> by silicate weathering can be significantly overestimated if acid  
428 deposition is ignored in short- and long-term perspectives. The result is important as it  
429 quantitatively shows that anthropogenic activities can significantly affect rock

430 weathering and associated atmospheric CO<sub>2</sub> consumption. The quantification of this  
431 effect needs to be well evaluated in Asian and global scale within the current and future  
432 human activity background.

## 433 **6. Conclusions**

434 River waters in the Southeast coastal region of China are characterized by high  
435 proportions of Na<sup>+</sup>, K<sup>+</sup> and dissolved SiO<sub>2</sub>, indicating water chemistry of the rivers in  
436 the SECRB is mainly controlled by silicate weathering. The dissolved cationic loads of  
437 the rivers in the study area originate dominantly from silicate weathering, which  
438 accounts for 39.5% (17.8-74.0%) of the total cationic loads. Carbonate weathering,  
439 atmospheric and anthropogenic inputs account for 30.6%, 14.3% and 15.7%,  
440 respectively. Meanwhile, more than 70% of SO<sub>4</sub><sup>2-</sup> in the rivers derived from  
441 atmospheric input. The chemical weathering rate of silicates and carbonates for the  
442 whole SECRB are estimated to be approximately 23.7 and 24.5 ton km<sup>-2</sup> a<sup>-1</sup>. About  
443 8.04×10<sup>6</sup> t a<sup>-1</sup> of dissolved solids originating from rock weathering are transported into  
444 the East and South China Sea by these rivers. With the assumption that all the protons  
445 involved in the weathering reaction are provided by carbonic acid, the CO<sub>2</sub>  
446 consumption rates by silicate and carbonate weathering are 287 and 251×10<sup>3</sup> mol km<sup>-2</sup>  
447 a<sup>-1</sup>, respectively. However, both water chemistry and carbon isotope data provide  
448 evidence that sulfuric acid from precipitation serves as a significant agent during  
449 chemical weathering. Considering the effect of sulfuric acid, the CO<sub>2</sub> consumption rate  
450 by silicate weathering for the SECRB are 218×10<sup>3</sup> mol km<sup>-2</sup> a<sup>-1</sup>. Therefore, the CO<sub>2</sub>  
451 consumption flux would be overestimated by 11.5×10<sup>9</sup> mol a<sup>-1</sup> (0.14×10<sup>12</sup> g C a<sup>-1</sup>) in

452 the SECRB if the effect of sulfuric acid is ignored. This work illustrates that  
453 anthropogenic disturbance by acid precipitation has profound impact on CO<sub>2</sub>  
454 sequestration by rock weathering.

455 **Acknowledgements.** This work was financially supported by Natural Science  
456 Foundation of China (Grant No. 41673020, 91747202, 41772380 and 41730857) and  
457 the "Strategic Priority Research Program" of the Chinese Academy of Sciences (Grant  
458 No. XDB15010405)

459 **References:**

460 Amiotte-Suchet, P., Probst, A. Probst, J.-L., Influence of acid rain on CO<sub>2</sub> consumption  
461 by rock weathering: local and global scales. *Water Air Soil Pollut.* 85, 1563-1568,  
462 1995.

463 Amiotte-Suchet, P., Probst, J.-L. Ludwig, W., Worldwide distribution of continental  
464 rock lithology: implications for the atmospheric/soil CO<sub>2</sub> uptake by continental  
465 weathering and alkalinity river transport to the oceans. *Global Biogeochem.*  
466 *Cycles* 17, 1038-1052, 2003.

467 Bai, H., Song, L.S., Xia, W.P., Prospect analysis of hot dry rock (HDR) in Eastern part  
468 of Jiangxi province, *Coal Geol. China* 26, 41-44. (In Chinese), 2014.

469 Berner, R.A., Caldeira, K., The need for mass balance and feedback in the geochemical  
470 carbon cycle. *Geology* 25, 955-956, 1997.

471 Bluth, G.J.S., Kump, L.R., Lithological and climatological controls of river chemistry.  
472 *Geochim. Cosmochim. Acta* 58, 2341-2359, 1994.

473 Brantley, S.L., Lebedeva, M., Learning to read the chemistry of regolith to understand

474 the Critical Zone. *Annual Review of Earth and Planetary Sciences*, 39: 387-416,  
475 2011.

476 Calmels, D., Gaillardet, J., Brenot, A., France-Lanord, C., Sustained sulfide oxidation  
477 by physical erosion processes in the Mackenzie River basin: climatic perspectives.  
478 *Geology* 35, 1003-1006, 2007.

479 Calmels, D., Galy, A., Hovius, N., Bickle, M., West, A.J., Chen, M.-C., Chapman, H.,  
480 Contribution of deep groundwater to the weathering budget in a rapidly eroding  
481 mountain belt, Taiwan. *Earth Planet. Sci. Lett.* 303, 48-58, 2011.

482 Cerling, T.E., Solomon, D.K., Quade, J., Bownman, J.R., On the isotopic composition  
483 of soil CO<sub>2</sub>. *Geochim. Cosmochim. Acta* 55, 3403–3405, 1991.

484 Chen, Q., Shen, C., Sun, Y., Peng, S., Yi, W., Li Z., Jiang, M., Spatial and temporal  
485 distribution of carbon isotopes in soil organic matter at the Dinghushan Biosphere  
486 Reserve, South China. *Plant and Soil*, 273: 115–128, 2005.

487 Cheng, Y., Liu, Y., Huo, M., Sun, Q., Wang, H., Chen, Z., Bai, Y., Chemical  
488 characteristics of precipitation at Nanping Mangdang Mountain in eastern China  
489 during spring. *J. Environ. Sci.* 23, 1350-1358, 2011.

490 Chetelat, B., Liu, C., Zhao, Z., Wang, Q., Li, S., Li, J., Wang, B., Geochemistry of the  
491 dissolved load of the Changjiang Basin rivers: anthropogenic impacts and  
492 chemical weathering. *Geochim. Cosmochim. Acta* 72, 4254-4277, 2008.

493 Cui, J., Zhou, J., Peng, Y., He, Y., Yang, H., Mao, J., Atmospheric wet deposition of  
494 nitrogen and sulfur to a typical red soil agroecosystem in Southeast China during  
495 the ten-year monsoon seasons (2003-2012). *Atmos. Environ.* 82, 121-129, 2014.

496 Das, A., Krishnaswami, S., Sarin, M.M., Pande, K., Chemical weathering in the Krishna  
497 Basin and Western Ghats of the Deccan Traps, India: Rates of basalt weathering  
498 and their controls. *Geochim. Cosmochim. Acta* 69(8), 2067-2084, 2005.

499 Dou, X., Deng, Q., Li, M., Wang, W., Zhang, Q., Cheng, X., Reforestation of *Pinus*  
500 *massoniana* alters soil organic carbon and nitrogen dynamics in eroded soil in  
501 south China. *Ecological Engineering* 52, 154-160, 2013.

502 Edmond, J.M., Palmer, M.R., Measures, C.I., Grant, B., Stallard, R.F., The fluvial  
503 geochemistry and denudation rate of the Guayana Shield in Venezuela, Colombia,  
504 and Brazil. *Geochim. Cosmochim. Acta* 59, 3301-3325, 1995.

505 Fan, B.L., Zhao, Z.Q., Tao, F.X., Liu, B.J., Tao, Z.H., Gao, S., He, M.Y., Characteristics  
506 of carbonate, evaporite and silicate weathering in Huanghe River basin: A  
507 comparison among the upstream, midstream and downstream. *J. Asian Earth Sci.*  
508 96, 17-26, 2014.

509 Fang, Y., Wang, X., Zhu, F., Wu, Z., Li, J., Zhong, L., Chen, D., Yoh, M., Three-decade  
510 changes in chemical composition of precipitation in Guangzhou city, southern  
511 China: has precipitation recovered from acidification following sulphur dioxide  
512 emission control? *Tellus B* 65, 1-15, 2013.

513 Faure, G., *Principles of Isotope Geology*. Wiley, Toronto, pp. 492-493, 1986.

514 FJBGMR: Fujian Bureau of Geology and Mineral Resources, *Regional Geology of*  
515 *Fujian Province*. Geol. Publ. House, Beijing, p. 671 (in Chinese with English  
516 abstract), 1985.

517 Gaillardet, J., Dupré, B., Allègre, C.J., Négrel, P., Chemical and physical denudation in

518 the Amazon River basin. *Chem. Geol.* 142, 141-173, 1997.

519 Gaillardet, J., Dupré, B., Louvat, P., Allegre, C.J., Global silicate weathering and CO<sub>2</sub>  
520 consumption rates deduced from the chemistry of large rivers. *Chem. Geol.* 159,  
521 3-30, 1999.

522 Galy, A., France-Lanord, C., Weathering processes in the Ganges-Brahmaputra basin  
523 and the riverine alkalinity budget. *Chem. Geol.* 159, 31-60, 1999.

524 Gandois, L., Perrin, A.-S., Probst, A., Impact of nitrogenous fertilizer-induced proton  
525 release on cultivated soils with contrasting carbonate contents: A column  
526 experiment. *Geochim. Cosmochim. Acta* 75, 1185-1198, 2011.

527 Gislason, S.R., Arnorsson, S., Armannsson, H., Chemical weathering of basalt in  
528 southwest Iceland: effects of runoff, age of rocks and vegetative/glacial cover.  
529 *Am. J. Sci.* 296, 837-907, 1996.

530 Han, G., Liu, C.Q., Water geochemistry controlled by carbonate dissolution: a study of  
531 the river waters draining karst-dominated terrain, Guizhou Province, China.  
532 *Chem. Geol.* 204, 1-21, 2004.

533 Han, Z.W., Ueda, H., Sakurai, T., Model study on acidifying wet deposition in East Asia  
534 during wintertime. *Atmos. Environ.* 40, 2360-2373, 2006.

535 Hartmann, J., Jansen, N., Dürr, H.H., Kempe, S., Köhler, P., Global CO<sub>2</sub> consumption  
536 by chemical weathering: what is the contribution of highly active weathering  
537 regions? *Global Planet. Change* 69, 185-194, 2009.

538 Huang, K., Zhuang, G., Xu, C., Wang Y., Tang A., The chemistry of the severe acidic  
539 precipitation in Shanghai, China. *Atmos. Res.* 89, 149-160, 2008.

540 Huh, Y.S., Chemical weathering and climate - a global experiment: a review. *Geosci. J.*  
541 7, 277-288, 2003.

542 Hydrological data of river basins in Zhejiang, Fujian province and Taiwan region,  
543 Annual Hydrological Report P. R. China, 2010, Vol (7) (in Chinese)

544 Ji, H., Jiang, Y., Carbon flux and C, S isotopic characteristics of river waters from a  
545 karstic and a granitic terrain in the Yangtze River system. *J. Asian Earth Sci.* 57,  
546 38-53, 2012.

547 Karim, A., Veizer, H.E., Weathering processes in the Indus River Basin: implication  
548 from riverine carbon, sulphur, oxygen and strontium isotopes. *Chem. Geol.* 170,  
549 153-177, 2000.

550 Kump, L.R., Brantley, S.L., Arthur, M.A., Chemical weathering, atmospheric CO<sub>2</sub> and  
551 climate. *Ann. Rev. Earth Planet. Sci.* 28, 611-667, 2000.

552 Larssen, T., Carmichael, G.R., Acid rain and acidification in China: the importance of  
553 base cation deposition. *Environ. Poll.* 110, 89-102, 2000.

554 Larssen, T., Lydersen, E., Tang, D., He, Y., Gao, J., Liu, H., Duan, L., Seip, H.M., Acid  
555 rain in China. *Environ. Sci. Technol.* 40, 418-425, 2006.

556 Lerman, A., Wu, L., CO<sub>2</sub> and sulfuric acid controls of weathering and river water  
557 composition. *J. Geochem. Explor.* 88, 427-430, 2006.

558 Lerman, A., Wu, L., Mackenzie, F.T., CO<sub>2</sub> and H<sub>2</sub>SO<sub>4</sub> consumption in weathering and  
559 material transport to the ocean, and their role in the global carbon balance. *Mar.*  
560 *Chem.* 106, 326-350, 2007.

561 Li, S., Bush, R.T., Changing fluxes of carbon and other solutes from the Mekong River.

562 Sci. Rep. 5, 16005, 2015.

563 Li, S.Y., Lu, X.X., Bush, R.T., Chemical weathering and CO<sub>2</sub> consumption in the Lower  
564 Mekong River. *Sci. Total Environ.* 472, 162-177, 2014.

565 Li, S.Y., Lu, X.X., He, M., Zhou, Y., Bei, R., Li, L., Zieglera, A.D., Major element  
566 chemistry in the Upper Yangtze River: a case study of the Longchuanjiang River.  
567 *Geomorphology* 129, 29-42, 2011.

568 Li, S.Y., Xu, Z.F., Wang, H., Wang, J.H., Zhang, Q.F., Geochemistry of the upper Han  
569 River basin, China. 3: anthropogenic inputs and chemical weathering to the  
570 dissolved load. *Chem. Geol.* 264, 89-95, 2009.

571 Liu, B., Liu, C.-Q., Zhang, G., Zhao, Z.-Q., Li, S.-L., Hu, J., Ding, H., Lang, Y.-C., Li.,  
572 X.-D., Chemical weathering under mid- to cool temperate and monsoon-  
573 controlled climate: A study on water geochemistry of the Songhuajiang River  
574 system, northeast China. *Appl. Geochem.* 31, 265-278, 2013.

575 Liu, L., Zhang, X., Wang, S., Zhang, W., Lu, X., Bulk sulfur (S) deposition in China.  
576 *Atmos. Environ.*, 135, 41-49, 2016.

577 Lu, Z., Zhang, Q., Streets, D.G., Sulfur dioxide and primary carbonaceous aerosol  
578 emissions in China and India, 1996e2010. *Atmos. Chem. Phys.* 11, 9839-9864,  
579 2011.

580 Millot, R., Gaillardet, J., Dupré, B., Allègre, C.J., Northern latitude chemical  
581 weathering rates: clues from the Mackenzie River Basin, Canada. *Geochim.*  
582 *Cosmochim. Acta* 67, 1305-1329, 2003.

583 Millot, R., Gaillardet, J., Dupré, B., Allègre, C.J., The global control of silicate

584 weathering rates and the coupling with physical erosion: new insights from rivers  
585 of the Canadian Shield. *Earth Planet. Sci. Lett.* 196, 83-98, 2002.

586 Moon, S., Chamberlain, C.P., Hilley, G.E., New estimates of silicate weathering rates  
587 and their uncertainties in global rivers. *Geochim. Cosmochim. Acta* 134, 257-274,  
588 2014.

589 Moon, S., Huh, Y., Qin, J., van Pho, N., Chemical weathering in the Hong (Red) River  
590 basin: Rates of silicate weathering and their controlling factors. *Geochim.*  
591 *Cosmochim. Acta* 71, 1411-1430, 2007.

592 Moon, S., Huh, Y., Zaitsev, A., Hydrochemistry of the Amur River: Weathering in a  
593 Northern Temperate Basin. *Aquat. Geochem.*, 15, 497-527, 2009.

594 Mortatti, J., Probst, J.L., Silicate rock weathering and atmospheric/soil CO<sub>2</sub> uptake in  
595 the Amazon basin estimated from river water geochemistry: seasonal and spatial  
596 variations. *Chem. Geol.* 197, 177-196, 2003.

597 Négrel, P., Allègre, C.J., Dupré, B., Lewin, E., Erosion sources determined by inversion  
598 of major and trace element ratios and strontium isotopic ratios in river water: the  
599 Congo Basin Case. *Earth Planet. Sci. Lett.* 120, 59-76, 1993.

600 Noh, H., Huh, Y., Qin, J., Ellis, A., Chemical weathering in the Three Rivers region of  
601 Eastern Tibet. *Geochim. Cosmochim. Acta* 73, 1857-1877, 2009.

602 Oliva, P., Viers, J., Dupré B., Chemical weathering in granitic environments. *Chem.*  
603 *Geol.* 202, 225-256, 2003.

604 Pan, Y., Wang, Y., Tang, G., Wu, D., Spatial distribution and temporal variations of  
605 atmospheric sulfur deposition in Northern China: insights into the potential

606 acidification risks. *Atmos. Chem. Phys.* 13, 1675-1688, 2013.

607 Pepin, E., Guyot, J.L., Armijos, E., Bazan, H., Fraizy, P., Moquet, J.S., Noriega, L.,  
608 Lavado, W., Pombosa, R. Vauchel, P., Climatic control on eastern Andean  
609 denudation rates (Central Cordillera from Ecuador to Bolivia). *J. S. Am. Earth*  
610 *Sci.* 44, 85-93, 2013.

611 Perrin, A.-S., Probst, A., Probst, J.-L., Impact of nitrogenous fertilizers on carbonate  
612 dissolution in small agricultural catchments: Implications for weathering CO<sub>2</sub>  
613 uptake at regional and global scales. *Geochim, Cosmochim. Acta* 72, 3105-3123,  
614 2008.

615 Probst, A., Gh'mari, A.El., Aubert, D., Fritz, B., McNutt, R., Strontium as a tracer of  
616 weathering processes in a silicate catchment polluted by acid atmospheric inputs,  
617 Strengbach, France. *Chem. Geol.* 170, 203-219, 2000.

618 Raymo, M.E., Ruddiman, W.F., Tectonic forcing of late Cenozoic climate. *Nature* 359,  
619 117-122, 1992.

620 Raymond, P. A., Oh, N.H., Turner, R.E., Broussard, W., Anthropogenically enhanced  
621 fluxes of water and carbon from the Mississippi River. *Nature* 451, 449-452, 2008.

622 Regnier, P., Friedlingstein, P., Ciais, P., Mackenzie, F.T.,...Thullner. M.,  
623 Anthropogenic perturbation of the carbon fluxes from land to ocean. *Nature*  
624 *Geosci.* 6, 597-607. 2013.

625 Reuss, J.O., Cosby, B.J., Wright, R.F., Chemical processes governing soil and water  
626 acidification. *Nature* 329, 27-32, 1987.

627 Roy, S., Gaillardet, J., Allègre, C.J., Geochemistry of dissolved and suspended loads of

628 the Seine river, France: anthropogenic impact, carbonate and silicate weathering.  
629 *Geochim. Cosmochim. Acta* 63, 1277-1292, 1999.

630 Ryu, J.S., Lee, K.S., Chang, H.W., Shin, H.S., Chemical weathering of carbonates and  
631 silicates in the Han River basin, South Korea. *Chem. Geol.* 247, 66-80, 2008.

632 Semhi, K., Amiotte Suchet, P., Clauer, N., Probst, J.-L., Impact of nitrogen fertilizers  
633 on the natural weathering-erosion processes and fluvial transport in the Garonne  
634 basin. *Appl. Geochem.* 15 (6), 865-874, 2000.

635 Shi, C., Chemical characteristics and weathering of rivers in the Coast of Southeast  
636 China (PhD Thesis). Institute of Geology and Geophysics, Chinese academy of  
637 sciences, Beijing, China. pp, 1-100 (in Chinese with English abstract), 2014.

638 Shin, W.-J., Ryu, J.-S., Park, Y., Lee, K.-S., Chemical weathering and associated CO<sub>2</sub>  
639 consumption in six major river basins, South Korea. *Geomorphology* 129, 334-  
640 341, 2011.

641 Shu, L.S., Zhou, X.M., Deng, P., Wang, B., Jiang, S.Y., Yu, J.H., Zhao, X.X., Mesozoic  
642 tectonic evolution of the Southeast China Block: New insights from basin  
643 analysis. *J. Asian Earth Sci.* 34(3), 376-391, 2009.

644 Spence, J., Telmer, K., The role of sulfur in chemical weathering and atmospheric CO<sub>2</sub>  
645 fluxes: Evidence from major ions,  $\delta^{13}\text{C}_{\text{DIC}}$ , and  $\delta^{34}\text{S}_{\text{SO}_4}$  in rivers of the Canadian  
646 Cordillera. *Geochim. Cosmochim. Acta* 69, 5441-5458, 2005.

647 Stallard, R.F., Edmond, J.M., Geochemistry of the Amazon. Precipitation chemistry and  
648 the marine contribution to the dissolved load at the time of peak discharge. *J.*  
649 *Geophys. Res.*, 86, 9844-9858, 1981.

650 U.S. Nat. Res. Council Comm., Basic Research Opportunities in Earth Science.  
651 Washington, DC: Nat. Acad. 154 pp., 2001.

652 Viers, J., Dupré, B., Braun, J.J., Freydier, R., Greenberg, S., Ngoupayou, J.N.,  
653 Nkamdjou, L.S., Evidence for non-conservative behavior of chlorine in humid  
654 tropical environments. *Aquat. Geochem.* 7, 127-154, 2001.

655 Vries, W.D., Reinds, G.J. Vel E., Intensive monitoring of forest ecosystems in Europe.  
656 2-Atmospheric deposition and its impacts on soil solution chemistry. *For. Ecol.*  
657 *Manage.* 174, 97-115, 2003.

658 Wang, T.J., Jin, L.S., Li, Z.K., Lam K.S., A modeling study on acid rain and  
659 recommended emission control strategies in China. *Atmos. Environ.* 34, 4467-  
660 4477, 2000.

661 West, A.J., Galy, A., Bickle, M., Tectonic and climatic controls on silicate weathering.  
662 *Earth Planet. Sci. Lett.* 235, 211-228, 2005.

663 Wu, W., Zheng, H., Yang, J., Luo, C., Zhou, B., Chemical weathering, atmospheric CO<sub>2</sub>  
664 consumption, and the controlling factors in a subtropical metamorphic-hosted  
665 watershed. *Chem. Geol.* 356, 141-150, 2013.

666 Xiang, L., Study on Coupling between Water and Carbon of Artificial Forests  
667 Communities in Subtropical Southern China. Master Dissertation, Institute of  
668 Geographical Sciences and Natural Sources, Chinese Academy of Sciences,  
669 China (in Chinese), 2006.

670 Xu, H., Bi, X-H., Feng, Y-C., Lin, F-M., Jiao, L., Hong, S-M., Liu, W-G., Zhang, X.-  
671 Y., Chemical composition of precipitation and its sources in Hangzhou, China.

672 Environ. Monit. Assess. 183:581-592, 2011.

673 Xu, Y., Wang C.Y., Zhao T., Using detrital zircons from river sands to constrain major  
674 tectono-thermal events of the Cathaysia Block, SE China. *J. Asian Earth Sci.* 124,  
675 1-13, 2016.

676 Xu, Z., Liu, C.-Q., Chemical weathering in the upper reaches of Xijiang River draining  
677 the Yunnan-Guizhou Plateau, Southwest China. *Chem. Geol.* 239, 83-95, 2007.

678 Xu, Z., Liu, C.-Q., Water geochemistry of the Xijiang basin rivers, South China:  
679 Chemical weathering and CO<sub>2</sub> consumption. *Appl. Geochem.* 25, 1603-1614,  
680 2010.

681 Yoshimura, K., Nakao, S., Noto, M., Inokura, Y., Urata, K., Chen, M., Lin, P.W.,  
682 Geochemical and stable isotope studies on natural water in the Taroko Gorge karst  
683 area, Taiwan - chemical weathering of carbonate rocks by deep source CO<sub>2</sub> and  
684 sulfuric acid. *Chem. Geol.* 177, 415-430, 2001.

685 Zhang, M., Wang, S., Wu, F., Yuan, X., Zhang, Y., Chemical compositions of wet  
686 precipitation and anthropogenic influences at a developing urban site in  
687 southeastern China. *Atmos. Res.* 84, 311-322, 2007a.

688 Zhang, S.R., Lu, X. X., Higgitt, D. L., Chen, C.T.A., Sun, H.-G., Han, J.T., Water  
689 chemistry of the Zhujiang (Pearl River): Natural processes and anthropogenic  
690 influences. *J. Geophys. Res.* 112, F01011, 2007b.

691 Zhao, W., An analysis on the changing trend of acid rain and its causes in Fujian  
692 Province. *Fujian Geogr.* 19, 1-5 (in Chinese), 2004.

693 Zhou, X.M., Li, W.X., Origin of Late Mesozoic igneous rocks in Southeastern China:

694 Implications for lithosphere subduction and underplating of mafic magmas.  
695 Tectonophysics 326(3-4), 269-287, 2000.

696 Zhou, X.M., Sun, T., Shen, W.Z., et al., Petrogenesis of Mesozoic granitoids and  
697 volcanic rocks in South China: A response to tectonic evolution. Episodes 29(1),  
698 26-33, 2006.

699 ZJBGMR: Zhejiang Bureau of Geology and Mineral Resources, Regional Geology of  
700 Zhejiang Province. Geol. Publ. House, Beijing, p. 617 (in Chinese with English  
701 abstract), 1989.

Table 1 Chemical and carbon isotopic compositions of river waters in the Southeast Coastal Rivers Basin (SECRB) of China.

Rivers	Sample number	Date (M/D/Y)	pH	T °C	EC $\mu\text{s cm}^{-1}$	Na <sup>+</sup> $\mu\text{M}$	K <sup>+</sup> $\mu\text{M}$	Mg <sup>2+</sup> $\mu\text{M}$	Ca <sup>2+</sup> $\mu\text{M}$	F <sup>-</sup> $\mu\text{M}$	Cl <sup>-</sup> $\mu\text{M}$	NO <sub>3</sub> <sup>-</sup> $\mu\text{M}$	SO <sub>4</sub> <sup>2-</sup> $\mu\text{M}$	HCO <sub>3</sub> <sup>-</sup> $\mu\text{M}$	SiO <sub>2</sub> $\mu\text{M}$	TZ <sup>+</sup> $\mu\text{Eq}$	TZ <sup>-</sup> $\mu\text{Eq}$	NICB %	$\delta^{13}\text{C}$ ‰	TDS $\text{mg l}^{-1}$
Qiantang	1	07-8-10	7.42	28.78	190	347	197	106	473	12.0	303	62.6	147	1130	148	1703	1789	-5.0	-19.0	144
	2	07-9-10	7.60	23.84	146	87.5	204	80.9	496	11.7	75.2	124	121	907	156	1446	1348	6.7	-19.8	119
	3	07-9-10	7.37	27.83	308	555	233	208	698	41.8	312	223	437	1170	170	2601	2579	0.9	-17.8	204
	4	07-10-10	7.27	26.28	177	176	135	116	544	15.7	151	142	170	985	175	1632	1618	0.8	-19.3	135
	5	07-10-10	7.05	24.15	123	130	101	66.2	349	17.7	94.3	124	157	529	169	1061	1061	0.0	-18.7	91.2
	6	07-10-10	7.24	23.75	140	97.6	69.7	81.0	451	20.0	62.1	109	204	703	164	1231	1282	-4.2	-21.3	106.6
	7	07-11-10	7.40	23.23	107	92.5	70.5	68.3	327	14.9	74.9	104	147	486	156	954	960	-0.6	-21.0	82.2
	8	07-11-10	7.16	27.61	281	361	87.5	128	469	26.8	245	191	239	810	179	1642	1724	-5.0	-12.9	137.5
	9	07-11-10	7.02	26.48	140	275	120	60.7	319	36.2	199	150	180	437	236	1155	1146	0.8	-13.9	100.2
	10	07-12-10	7.05	24.24	99	205	114	58.3	285	14.6	191	114	132	305	278	1005	874	13.1	-20.9	85.4
	11	07-12-10	7.05	27.01	102	123	133	49.8	284	18.6	86.5	123	144	377	183	924	874	5.4	-19.2	79.4
	12	07-12-10	7.99	24.18	260	50.0	85.4	212	993	-	66.8	153	235	1822	172	2546	2512	1.4	-17.6	205.2
	13	07-12-10	7.86	24.59	231	43.5	88.4	189	859	-	55.1	97.6	169	1763	170	2228	2253	-1.1	-18.7	185.4
	14	07-12-10	7.69	22.66	131	44.1	81.0	113	458	-	19.1	95.2	107	920	143	1266	1248	1.4	-18.1	106.8
	15	07-12-10	7.65	24.48	106	61.1	98.3	87.9	335	-	37.2	68.3	112	663	164	1005	992	1.4	-18.6	87.3
	16	07-12-10	7.46	23.68	125	64.3	108	117	406	-	25.9	75.0	174	687	164	1218	1136	6.7	-20.0	98.8
	17	07-13-10	7.33	24.08	139	59.8	116	136	429	-	29.6	80.4	209	752	162	1305	1281	1.9	-20.8	108.1
	18	07-10-10	7.27	25.74	141	163	114	69.6	396	27.3	126	148	161	597	153	1209	1195	1.1	-21.0	101.0
Cao'e	19	07-16-10	7.17	22.27	108	212	86.3	69.4	183	5.1	151	148	114	384	216	803	912	-13.5	-21.2	79.1
	20	07-16-10	7.06	26.57	182	401	77.6	145	275	18.3	269	185	245	534	215	1318	1478	-12.2	-20.5	116.9
	21	07-16-10	7.14	27.26	171	333	91.3	164	362	18.1	224	194	207	658	225	1475	1490	-1.0	-20.9	123.3
	22	07-16-10	7.08	27.17	173	346	94.4	168	364	18.8	247	200	211	656	222	1506	1526	-1.3	-13.0	125.2
Ling	23	07-15-10	7.07	24.14	52	164	42.9	34.9	140	4.9	40.7	61.5	68.3	277	190	558	516	7.6	-12.8	52.1
	24	07-15-10	7.02	26.04	74	169	92.0	34.2	150	6.4	87.0	77.3	92.8	272	196	629	622	1.1	-20.8	59.5
	25	07-16-10	7.34	25.03	92	159	80.1	47.3	235	19.3	78.0	71.4	105	455	187	804	815	-1.4	-22.5	73.9
	26	07-16-10	7.40	26.75	113	216	77.8	57.1	249	20.2	133	90.0	115	494	196	905	946	-4.5	-12.7	82.8
	27	07-16-10	7.39	26	89	174	86.4	56.4	209	9.0	99.3	78.4	99.9	420	199	792	798	-0.8	-14.0	72.7
	28	07-15-10	6.79	22.33	75	159	82.7	44.1	143	-	107	61.8	83.4	306	144	616	641	-4.1	-21.1	56.5
	29	07-15-10	8.24	27.15	129	228	92.1	83.1	317	17.2	177	90.5	120	641	194	1120	1148	-2.5	-19.2	97.8
Ou	30	07-13-10	8.08	28.45	48	95.2	107	38.4	92.1	15.2	31.8	43.3	47.4	291	221	463	461	0.4	-21.7	50.6
	31	07-13-10	6.71	22.97	32	60.7	106	12.6	65.0	10.8	28.9	45.0	48.9	158	169	322	329	-2.2	-23.8	36.9
	32	07-13-10	7.18	27.59	73	107	127	36.2	175	4.3	57.1	111	92.0	283	210	655	634	3.2	-23.4	62.9
	33	07-13-10	6.94	24.2	44	76.9	112	20.0	99.1	10.9	27.9	63.1	58.6	249	184	427	457	-7.0	-22.5	47.5
	34	07-14-10	7.16	27.45	90	187	127	41.2	199.5	17.0	85.6	102	116	367	251	796	787	1.1	-22.4	76.5
	35	07-14-10	6.97	24.56	54	105	50.9	29.2	122	12.2	46.1	67.8	73.1	218	193	460	478	-4.1	-22.5	47.9
	36	07-14-10	6.82	21.12	31	76.4	133	12.7	74.5	7.7	20.7	36.8	49.1	192	162	383	348	9.3	-	39.5
	37	07-14-10	6.82	23.69	45	89.5	105	19.0	97.8	10.6	39.6	52.8	59.1	231	185	428	441	-3.0	-22.9	46.2
	38	07-15-10	6.92	24.69	37	100	89.3	21.1	49.7	1.7	36.9	45.5	52.7	153	202	331	341	-2.9	-	38.9
	39	07-15-10	6.90	23.86	35	92.2	92.0	19.8	61.4	1.9	43.9	47.9	55.5	139	193	347	342	1.4	-22.3	38.5
	40	07-15-10	7.09	25.56	47	117	112	25.7	83.4	8.0	52.4	63.1	57.4	232	193	447	462	-3.3	-22.5	48.1
	41	07-14-10	6.97	24.25	53	102	107	27.6	119	13.4	43.5	59.4	73.2	277	183	502	526	-4.9	-13.7	52.3

Feiyun	42	07-17-10	7.28	25.19	38	94.0	81.7	24.0	75.6	11.4	59.9	45.7	51.9	149	151	375	358	4.5	-	37.2
	43	07-17-10	7.08	25.61	46	101	79.9	33.9	93.4	4.6	66.2	55.1	52.8	223	151	435	450	-3.3	-23.7	43.5
Jiaoxi	44	07-17-10	7.52	26.92	47	116	81.5	25.2	92.0	4.1	73.3	80.3	25.0	226	151	432	430	0.5	-23.4	43.0
	45	07-17-10	7.45	27.46	61	152	90.2	34.2	119	-	136	59.8	53.5	238	184	548	542	1.2	-23.1	51.8
	46	07-18-10	6.90	27.66	53	127	88.1	33.4	94.4	7.0	123	93.1	30.4	209	177	471	486	-3.3	-14.4	47.4
Huotong	47	07-18-10	7.34	24	43	116	78.8	26.1	58.4	5.4	68.7	49.7	20.1	197	190	364	355	2.3	-22.8	39.6
Ao	48	07-19-10	7.24	31.44	124	294	121	102	209	24.3	204	73.6	52.0	717	370	1036	1100	-6.1	-19.4	105.4
	49	07-19-10	7.13	27.82	46	109	96.3	30.0	73.8	-	72.0	51.3	22.5	234	236	413	402	2.6	-	46.2
	50	07-18-10	6.98	28.65	53	140	88.4	40.8	100	3.0	82.9	58.6	20.9	294	233	511	477	6.6	-22.3	52.2
Min	51	07-27-10	7.11	28.4	42	116	92.0	40.5	119	18.0	43.9	35.5	26.0	382	182	526	513	2.4	-19.4	52.7
	52	07-27-10	7.17	30	51	102	97.9	41.7	107	4.6	29.4	45.3	35.0	350	221	496	495	0.2	-	53.3
	53	07-27-10	7.08	29.4	99	214	92.7	46.4	126	18.4	50.1	39.8	118	327	154	651	654	-0.4	-20.8	74.0
	54	07-27-10	7.06	29.1	44	107	99.6	28.1	114	16.4	18.7	36.4	44.3	305	265	491	449	8.5	-17.6	53.6
	55	07-27-10	7.42	29.4	57	139	93.7	49.8	113	3.1	67.1	56.3	26.6	384	236	558	561	-0.5	-16.4	58.6
	56	07-27-10	7.12	27.8	51	103	91.0	50.8	106	4.7	82.8	35.1	63.5	249	225	507	494	2.5	-	51.3
	57	07-27-10	7.08	27.5	40	125	45.0	36.8	107	12.1	43.6	44.5	29.3	288	211	457	435	5.0	-21.1	47.4
	58	07-27-10	6.99	27.2	52	121	98.0	42.4	115	16.7	87.1	36.6	70.9	277	228	535	542	-1.4	-11.4	55.3
	59	07-27-10	6.87	29	59	154	91.4	59.4	124	16.5	77.8	36.7	88.3	272	222	612	563	8.0	-20.3	57.2
	60	07-27-10	7.31	27.1	78	109	92.1	59.1	181	21.2	123	37.5	78.4	355	202	682	672	1.4	-18.7	63.1
	61	07-27-10	7.22	27.8	37	122	83.3	52.8	142	17.4	111	37.3	80.4	288	221	596	597	-0.2	-22.3	58.1
	62	07-27-10	7.16	28.1	58	104	83.3	59.3	163	24.0	34.6	34.5	118	294	214	632	599	5.2	-13.4	59.5
	63	07-27-10	7.26	28.3	87	139	86.1	60.9	191	14.8	48.0	93.0	109	347	226	729	707	3.0	-21.4	68.6
	64	07-27-10	7.00	28.8	87	127	93.1	58.7	195	6.6	59.8	81.1	60.9	480	232	729	743	-2.0	-11.0	74.0
	65	07-28-10	6.97	27.9	37	163	82.1	52.2	140	20.2	53.1	60.0	106	306	221	630	632	-0.2	-	61.9
	66	07-13-10	7.07	27.96	59	91.9	110	40.0	127	24.8	62.0	79.3	62.3	249	228	535	515	3.8	-	54.8
	67	07-28-10	7.12	29.7	38	108	93.4	45.9	133	12.4	48.3	34.0	56.6	368	220	560	564	-0.7	-	57.7
	68	07-27-10	7.03	29.9	62	128	96.7	57.6	148	23.3	81.6	36.8	74.1	374	203	635	641	-0.9	-12.4	61.7
	69	07-27-10	7.01	28.8	60	102	89.1	73.6	138	9.6	50.6	74.1	32.7	417	233	615	607	1.3	-21.0	62.3
	70	07-27-10	7.06	26.5	37	93.5	93.1	34.7	87.3	-	26.6	34.8	37.1	312	222	431	448	-3.9	-13.1	49.1
	71	07-27-10	7.09	26.5	25	62.6	92.7	27.0	61.5	4.7	21.5	18.6	43.4	191	154	332	318	4.2	-16.0	35.3
	72	07-28-10	7.07	30.1	39	76.3	87.9	35.1	87.6	7.4	43.1	36.6	35.5	266	175	409	416	-1.7	-19.4	43.5
	73	07-27-10	7.01	28.7	47	84.9	95.4	56.7	106	12.7	51.8	49.2	57.2	315	211	506	531	-4.8	-	53.8
	74	07-27-10	6.85	28.7	50	93.6	85.9	52.4	107	14.1	62.8	57.5	57.0	252	217	498	487	2.2	-19.9	50.9
	75	07-27-10	7.11	29.7	69	117	85.2	73.4	159	7.6	63.7	75.2	47.4	418	230	666	652	2.2	-22.2	65.0
	76	07-28-10	6.93	28.9	59	112	88.0	61.8	122	6.0	57.4	89.3	42.0	349	224	568	580	-2.2	-22.0	58.8
	77	07-21-10	7.76	32.4	51.2	163	85.5	52.8	151	20.2	55.3	70.3	78.6	372	175	656	655	0.3	-12.5	61.8
	78	07-28-10	7.29	26.8	106	129	75.3	84.0	321	24.0	56.2	41.0	166	599	202	1013	1028	-1.4	-16.3	90.3
	79	07-21-10	7.09	26.96	56	112	87.6	37.1	129	4.5	51.5	44.9	61.9	327	276	531	547	-2.9	-22.2	59.1
	80	07-21-10	7.64	33.37	83	114	96.2	60.6	151	16.7	53.0	40.6	102	371	242	633	670	-5.8	-12.8	66.2
	81	07-21-10	7.83	31.27	65	131	102	52.7	141	16.1	45.3	49.7	91.8	324	239	620	603	2.8	-13.4	61.8
	82	07-21-10	6.84	28.35	66	132	101	52.5	141	5.8	63.8	54.1	91.6	304	243	621	606	2.5	-22.7	61.5
	83	07-21-10	7.42	30.7	98	217	113	59.2	210	18.4	98.7	63.5	84.7	496	320	868	827	4.6	-18.9	84.5
	84	07-27-10	7.26	26.3	46	104	102	29.7	121	3.6	55.2	51.9	55.5	294	193	507	512	-0.9	-21.6	51.9
	85	07-27-10	7.07	25.4	30	73.3	99.2	19.6	78.8	-	22.9	40.0	49.2	203	170	369	365	1.3	-21.1	39.8
	86	07-27-10	7.50	27.3	45	102	102	26.5	114	2.4	35.1	39.7	57.2	260	217	484	449	7.3	-15.7	49.6
	87	07-27-10	7.47	26.9	51	141	100	43.6	109	7.9	79.7	42.4	57.7	311	217	547	548	-0.3	-20.1	55.6

	88	07-19-10	7.99	31.74	63	167	96.5	33.5	115	8.0	105	35.5	38.1	331	218	561	548	2.3	-13.5	55.9
	89	07-21-10	6.77	28.19	65	132	93.6	56.0	145	15.6	60.6	78.8	75.4	333	243	627	624	0.5	-22.6	63.3
Jin	90	07-27-10	7.36	25.8	128	126	94.8	88.9	406	22.9	51.4	39.4	229	595	208	1211	1143	5.6	-20.7	100
	91	07-27-10	7.40	26.9	123	143	103	82.7	347	21.0	83.5	203	182	463	226	1105	1115	-0.9	-21.3	98.4
	92	07-27-10	7.00	27.4	88	170	98.8	56.8	205	7.2	137	117	106	327	205	793	792	0.1	-22.5	71.8
	93	07-27-10	7.32	28.7	73	201	116	87.1	318	20.0	93.5	41.5	189	508	267	1128	1020	9.6	-21.7	95.3
Jiulong	94	07-30-10	6.50	23.47	29	72.3	92.4	22.8	59.8	12.4	25.1	27.0	50.0	189	213	330	341	-3.4	-18.1	40.1
	95	07-30-10	7.06	29.35	120	136	96.9	106	339	5.1	67.7	66.3	249	469	202	1124	1100	2.1	-20.8	94.2
	96	07-30-10	7.45	27.6	104	79.5	97.5	106	363	14.4	70.7	50.0	99.9	729	184	1116	1049	6.0	-18.9	93.7
	97	07-31-10	7.36	26.59	139	140	100	142	432	15.5	79.6	78.3	274	573	196	1388	1278	8.0	-19.7	108.8
	98	07-31-10	7.72	26.18	88	77.6	96.2	69.0	313	19.9	39.7	34.6	63.8	731	251	938	933	0.5	-18.4	89.4
	99	07-30-10	7.43	26.96	119	200	93.8	100.2	298	19.9	122	80.5	225	387	202	1091	1040	4.7	-20.5	89.5
	100	07-28-10	7.41	26.66	112	173	97.9	94.4	286	46.1	118	152	201	364	207	1033	1036	-0.3	-20.9	92.2
	101	07-29-10	7.16	29.35	82	151	110	55.4	178	4.9	71.2	170	53.2	385	305	727	732	-0.7	-21.2	76.1
	102	07-29-10	7.10	28.9	100	222	98.3	49.4	249	3.6	126	157	52.7	532	303	917	920	-0.3	-21.7	90.0
	103	07-28-10	7.20	31.15	138	339	111	81.2	277	9.2	280	285	88.6	515	317	1165	1256	-7.8	-19.0	112
	104	07-28-10	7.16	27.09	101	261	95.8	81.7	235	40.3	173	80.1	174	291	136	990	892	9.9	-24.3	75.4
Zhang	105	07-28-10	8.08	30.6	93	195	96.1	61.1	167	16.8	157	193	55.2	281	288	748	741	0.9	-21.5	73.8
Dongxi	106	07-28-10	7.20	30.9	78	263	99.0	41.5	115	14.5	238	65.3	30.0	283	309	675	646	4.4	-20.8	66.7
Huangang	107	07-28-10	7.40	30.5	99	253	85.6	53.0	154	7.7	190	63.5	56.4	460	278	754	827	-9.6	-20.0	77.4
Han	108	07-31-10	7.31	27.1	68	136	61.5	45.2	195	16.1	37.7	45.3	93.7	345	218	678	615	9.2	-21.9	62.0
	109	07-30-10	7.38	26.94	88	116	103	63.6	265	6.4	53.4	72.2	84.9	584	244	876	879	-0.4	-20.4	83.7
	110	07-30-10	6.66	25.55	71	114	96.2	47.6	168	8.0	56.9	54.6	143	230	203	642	628	2.2	-17.9	59.7
	111	07-30-10	6.66	27.76	83	135	104	63.8	203	8.6	54.5	74.9	173	302	336	774	777	-0.4	-20.6	78.7
	112	07-30-10	7.31	30.81	56	168	74.0	39.1	118	13.5	62.9	44.4	81.4	237	245	556	507	8.8	-21.4	54.6
	113	07-31-10	7.28	28.73	98	137	99.3	85.6	270	9.2	88.8	59.1	118	565	233	948	949	-0.1	-19.7	86.6
	114	07-31-10	7.27	31.42	123	193	105	98.2	319	20.7	120	102	157	570	229	1132	1107	2.2	-19.7	98.2
	115	07-30-10	7.43	29.89	85	115	97.5	65.5	244	6.5	46.5	58.6	103	511	251	832	822	1.1	-20.8	79.3
	116	07-31-10	7.61	30.98	99	123	104	85.9	264	5.6	58.8	90.9	108	588	98	926	952	-2.9	-20.0	79.4
	117	07-31-10	7.31	29.96	93	151	103	78.1	250	15.4	68.0	99.1	173	379	233	909	891	1.9	-21.9	81.8
	118	07-31-10	7.35	28.4	2	233	84.2	101	323	12.8	84.0	101	203	460	229	1165	1051	9.8	-21.1	94.7
	119	07-31-10	7.67	30.38	93	136	87.8	73.6	231	16.4	64.6	94.4	184	382	226	834	909	-9.1	-20.8	80.5
Rong	120	07-30-10	7.57	31.83	68	193	79.1	50.3	146	16.4	192	84.0	31.5	344	309	664	683	-2.8	-20.3	65.8
	121	07-30-10	6.96	30.62	94	509	103	56.1	213	15.9	511	78.5	82.3	379	222	1150	1133	1.5	-20.0	94.4

TZ<sup>+</sup> is the total cationic charge; TZ<sup>-</sup> is the total anionic charge; NICB is the normalized inorganic charge balance and TDS is the total dissolved solid.

Table 2 Chemical compositions of precipitation at different sites located within the studied area (in  $\mu\text{mol l}^{-1}$  and molar ratio).

Province	Location	pH	F <sup>-</sup>	Cl <sup>-</sup>	NO <sub>3</sub> <sup>-</sup>	SO <sub>4</sub> <sup>2-</sup>	NH <sub>4</sub> <sup>+</sup>	K <sup>+</sup>	Na <sup>+</sup>	Ca <sup>2+</sup>	Mg <sup>2+</sup>	NO <sub>3</sub> /Cl	SO <sub>4</sub> /Cl	K/Cl	Na/Cl	Ca/Cl	Mg/Cl	Reference	
Zhejiang	Hangzhou	4.5	5.76	13.9	38.4	55	79.9	4.18	12.2	26	3.53	2.76	3.96	0.3	0.88	1.87	0.25	Xu et al., 2011	
	Jinhua	4.54	9.05	8.51	31.2	47.6	81.1	4.73	6.27	24	1.73	3.67	5.59	0.56	0.74	2.81	0.2	Zhang et al., 2007	
Fujian	Nanping	4.81	0.8	5.8	26.6	18.3	38	4.9	5.4	12.9	2.7	4.59	3.16	0.84	0.93	2.22	0.47	Cheng et al., 2011	
	Fuzhou		5.26	21.4	24.9	48.5	78.1	4.1	2.61	32.7	1.25	1.16	2.26	0.19	0.12	1.53	0.06	Zhao, 2004	
	Xiamen	4.57	15.3	23.7	22.1	31.3	37.7	3.58	36.1	21.5	4.94	0.93	1.32	0.15	1.52	0.91	0.21	Zhao, 2004	
Average												2.62	3.26	0.41	0.84	1.87	0.24		

Table 3 Contribution of each reservoir, fluxes, chemical weathering and associated CO<sub>2</sub> consumption rates for the major rivers and their main tributaries in the SECRB.

Major river	Tributaries	Location	Discharge 10 <sup>9</sup> m <sup>3</sup> a <sup>-1</sup>	Area 10 <sup>3</sup> km <sup>2</sup>	Runoff mm a <sup>-1</sup>	Contribution (%)				Fluxes (10 <sup>6</sup> ton a <sup>-1</sup> )		Weathering rate (ton km <sup>2</sup> a <sup>-1</sup> )				CO <sub>2</sub> consumption rate (10 <sup>3</sup> mol km <sup>2</sup> a <sup>-1</sup> )		
						Rain	Anth.	Sil.	Carb.	SWF	CWF	Cat <sub>sil</sub> <sup>a</sup>	SWR <sup>b</sup>	CWR <sup>b</sup>	TWR <sup>b</sup>	CSW <sup>c</sup>	CCW <sup>c</sup>	SSW <sup>d</sup>
Qiantang	Fuyang		43.81	38.32	1143	9	14	23	54	0.66	1.74	6.8	17.3	45.3	62.6	223	459	195
	Fenshui	Tonglu	2.726	3.100	879	7	14	18	62	0.05	0.16	5.5	14.7	52.1	66.8	167	530	152
Cao'e		Huashan	2.610	3.043	858	7	23	26	44	0.06	0.11	6.8	18.2	35.4	53.5	269	369	240
Ling		Linhai	5.400	6.613	817	9	22	24	45	0.09	0.17	4.7	14.2	26.1	40.3	167	267	143
	Yonganxi	Baizhiao	3.184	2.475	1286	14	15	50	21	0.06	0.03	9.1	24.2	11.7	35.9	350	119	255
	Shifengxi	Shaduan	1.731	1.482	1168	11	19	35	36	0.03	0.04	7.6	21.4	24.5	45.9	304	249	249
Ou		Hecheng	20.65	13.45	1536	20	6	56	18	0.36	0.13	10.1	26.9	9.9	36.9	360	101	228
	Haoxi	Huangdu	1.809	1.270	1447	16	8	46	30	0.04	0.02	9.9	27.9	19.0	46.9	336	192	246
	Xiaoxi	Jupu	5.116	3.336	1534	23	0	74	4	0.09	0.01	11.4	26.4	1.8	28.2	391	18	202
	Nanxi	Yongjiashi	1.799	1.273	1413	21	9	63	7	0.03	0.00	10.0	26.3	3.3	29.6	360	34	200
Huotong		Yangzhong	3.470	2.082	1667	22	18	54	5	0.06	0.00	8.3	27.3	2.1	29.4	305	24	129
Aojiang		Lianjiang	2.770	3.170	874	17	17	48	17	0.05	0.02	5.1	17.3	5.4	22.7	188	56	122
Minjiang		Zhuqi	84.59	54.50	1552	15	10	48	27	1.80	0.94	10.3	33.0	17.3	50.2	390	180	292
	Futun	Yangkou	22.53	12.67	1778	15	14	49	22	0.45	0.21	12.0	35.8	16.2	52.0	460	171	336
	Shaxi	Shaxian	12.87	9.922	1297	13	9	42	36	0.26	0.21	8.4	26.5	21.7	48.1	315	222	249
	Jianxi	Qilijie	24.91	14.79	1685	16	10	45	29	0.48	0.26	9.6	32.2	17.4	49.6	350	185	250
	Youxi	Youxi	5.237	4.450	1177	15	8	46	31	0.11	0.07	7.4	24.5	15.0	39.5	272	156	205
	Dazhangxi	Yongtai	4.205	4.034	1042	15	21	47	17	0.08	0.03	6.6	20.2	7.1	27.4	242	73	163
Jinjiang	Xixi	Anxi	3.004	2.466	1218	9	10	29	52	0.06	0.10	7.9	24.4	42.2	66.6	284	430	247
	Dongxi	Honglai	2.236	1.704	1312	12	22	28	38	0.04	0.04	6.8	22.9	25.6	48.5	226	263	178
Jiulong		Punan	10.20	8.49	1201	13	14	28	45	0.19	0.29	7.3	22.2	34.0	56.2	263	351	209
	Xi'xi	zhengdian	4.080	3.420	1193	10	32	25	33	0.10	0.11	8.0	30.7	30.9	61.6	288	317	227
Zhang		Yunxiao	1.011	1.038	974	16	25	29	29	0.02	0.01	5.1	21.9	14.1	36.0	174	146	114
Dongxi		Zhao'an	1.176	0.955	1231	16	41	26	17	0.03	0.01	5.8	28.7	10.2	38.9	187	107	93
Huanggang		Raoping	1.637	1.621	1010	15	30	34	21	0.04	0.02	6.0	22.8	11.1	33.9	227	115	145

Han	Chao'an	24.75	29.08	851	16	7	38	39	0.49	0.50	5.4	17.0	17.0	34.0	208	176	156	
	Ding	Xikou	11.14	9.228	1207	17	6	46	32	0.31	0.18	9.0	33.3	19.1	52.4	341	196	249
	Mei	Hengshan	10.29	12.95	794	12	13	31	44	0.21	0.32	5.7	16.6	24.5	41.1	212	252	173
Whole SECRB			207	167	1240					3.95	4.09	7.8	23.7	24.5	48.1	287	251	218

<sup>a</sup> Cat<sub>sil</sub> are calculated based on the sum of cations from silicate weathering.

<sup>b</sup> SWR, CWR and TWR represent silicate weathering rates (assuming all dissolved silica is derived from silicate weathering), carbonate weathering rates and total weathering rates, respectively.

<sup>c</sup> CO<sub>2</sub> consumption rate with assumption that all the protons involved in the weathering reaction are provided by carbonic acid.

<sup>d</sup> Estimated CO<sub>2</sub> consumption rate by silicate weathering when H<sub>2</sub>SO<sub>4</sub> originating from acid precipitation is taken into account.

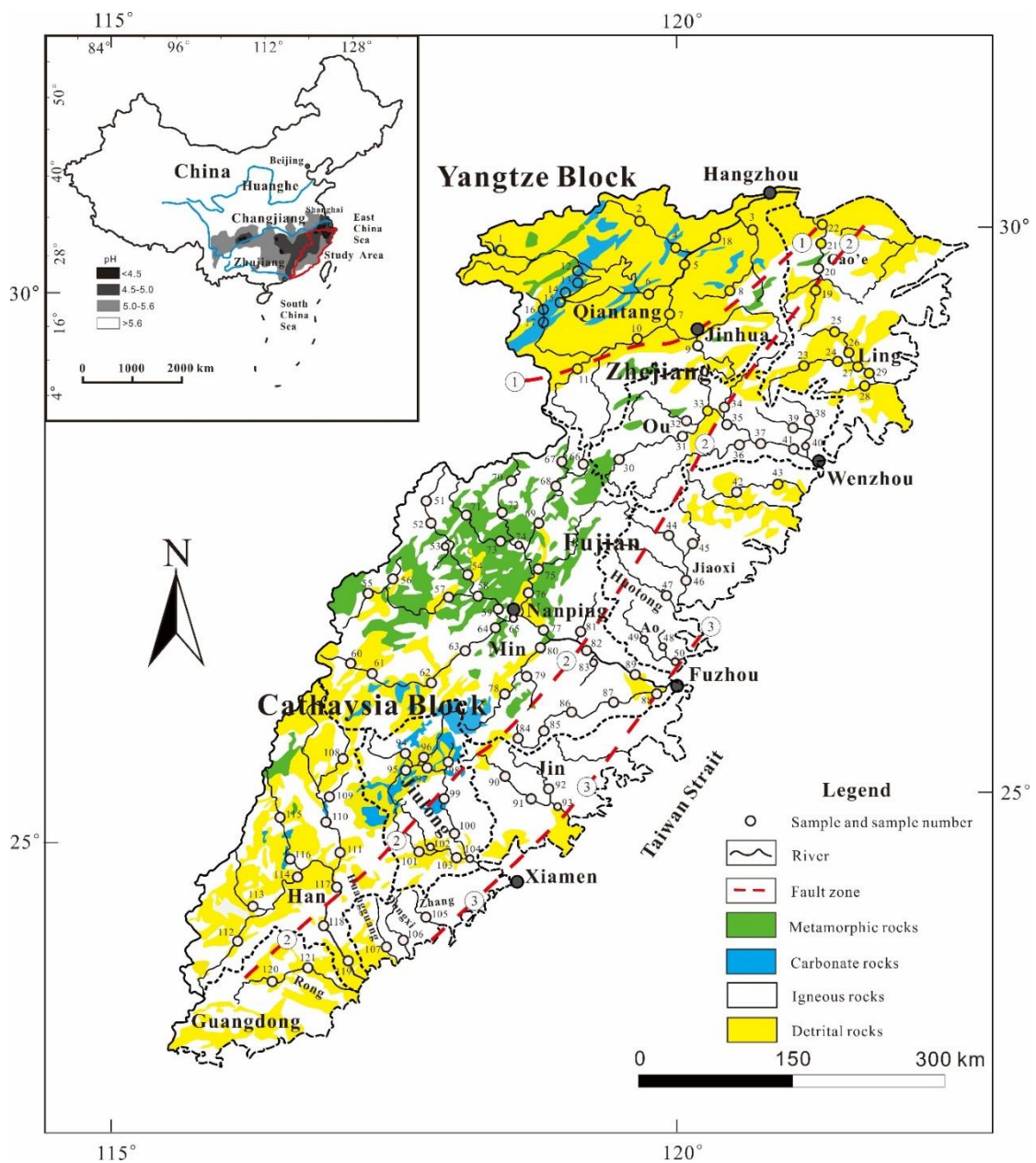


Fig. 1. Sketch map showing the lithology, sampling locations, and sample number of the SECRs drainage basin, and regional rain water pH ranges are shown in the sketch map at the upper-left. (modified from Zhou and Li, 2000; Shu et al., 2009; Xu et al., 2016, rain water acidity distribution of China mainland is from State Environmental Protection Administration of China). ①Shaoxing-Jiangshan fault zone; ②Zhenghe-Dapu fault zone; ③Changle-Nanao fault zone. The figure was created by CorelDraw software version 17.1.

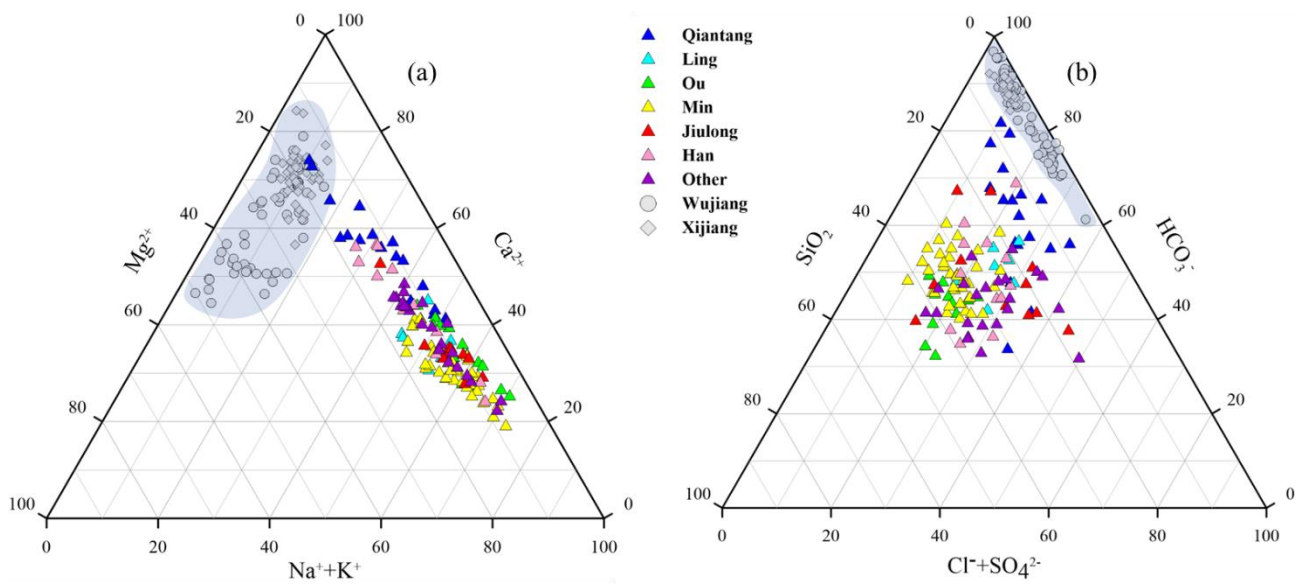


Fig. 2. Ternary diagrams showing cations (a), anions and dissolved  $SiO_2$  (b) compositions of river waters in the SECRB. Chemical compositions from case studies of rivers draining carbonate rocks (the Wujiang and the Xijiang) are also shown for comparison (data from Han and Liu 2004; Xu and Liu 2007, 2010)

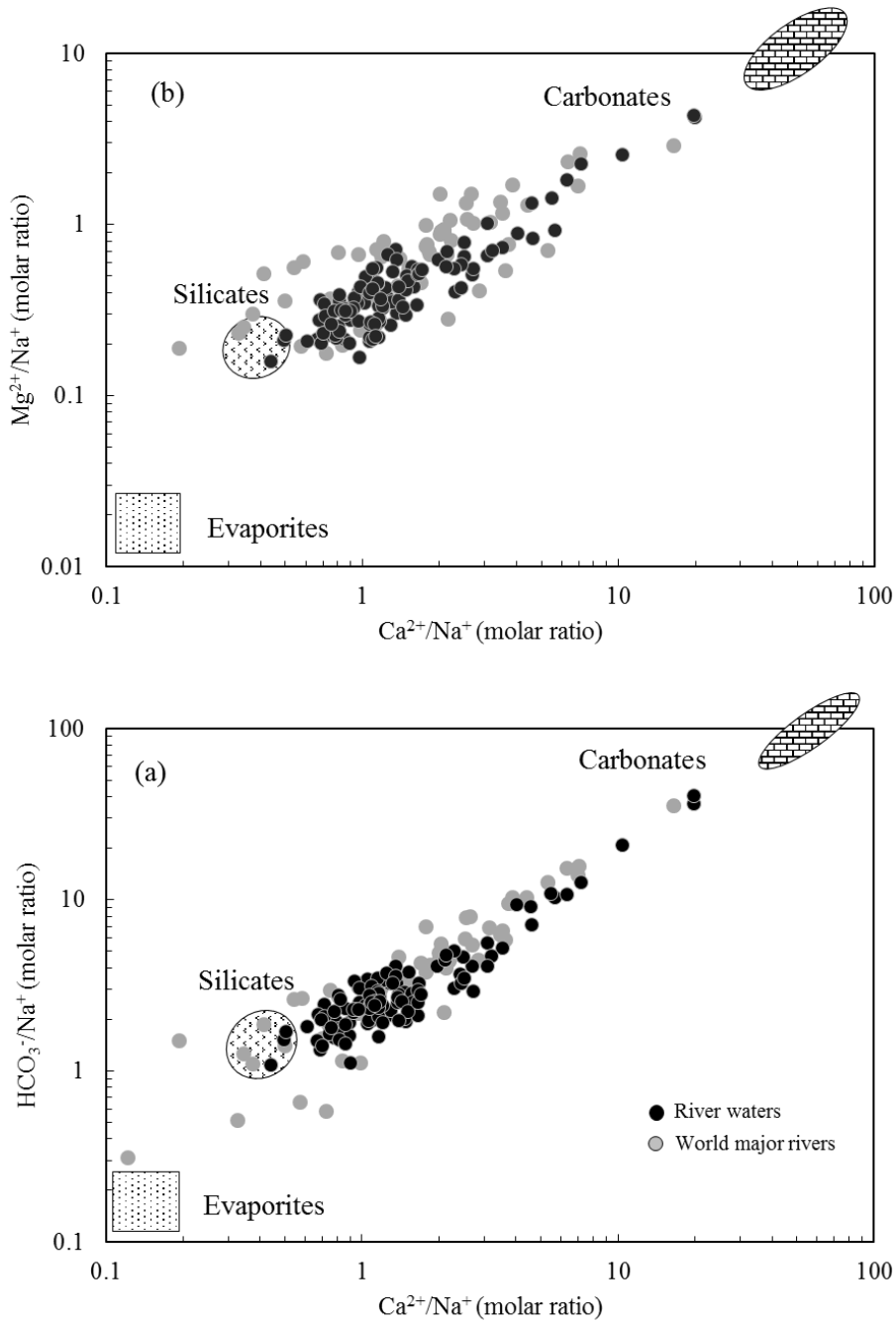


Fig. 3. Mixing diagrams using Na-normalized molar ratios:  $\text{HCO}_3^-/\text{Na}^+$  vs.  $\text{Ca}^{2+}/\text{Na}^+$  (a) and  $\text{Mg}^{2+}/\text{Na}^+$  vs.  $\text{Ca}^{2+}/\text{Na}^+$  (b) for the SECRB. The samples mainly cluster on a mixing line between silicate and carbonate end-members. Data for world major rivers are also plotted (data from Gaillardet et al. 1999).

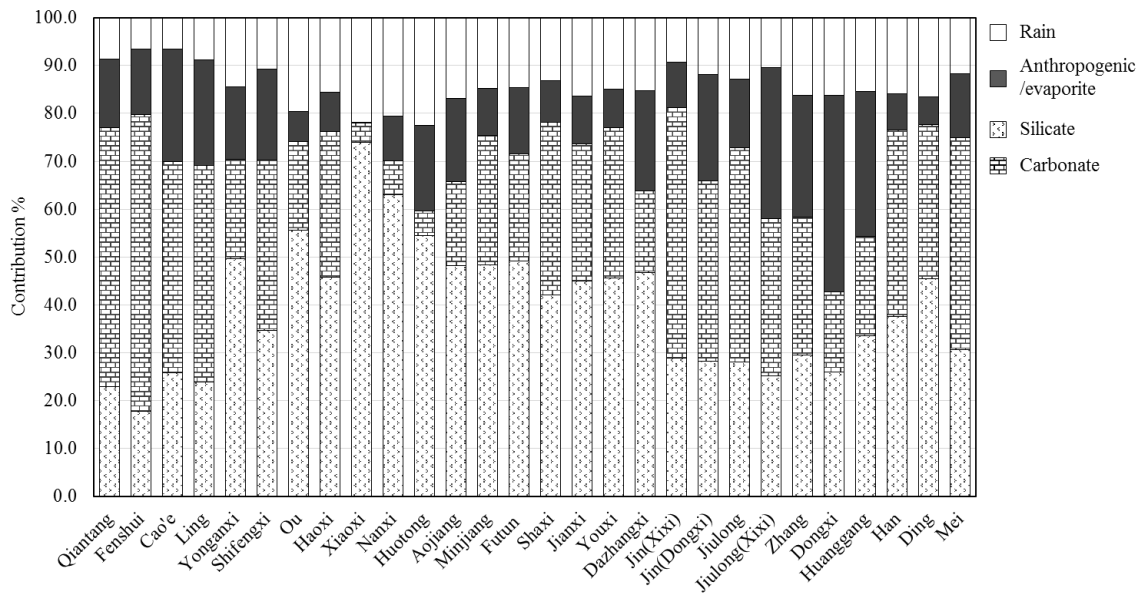


Fig. 4. Calculated contributions (in %) from the different reservoirs to the total cationic load for major rivers and their main tributaries in the SECRB. The cationic load is equal to the sum of  $\text{Na}^+$ ,  $\text{K}^+$ ,  $\text{Ca}^{2+}$  and  $\text{Mg}^{2+}$  from the different reservoirs.

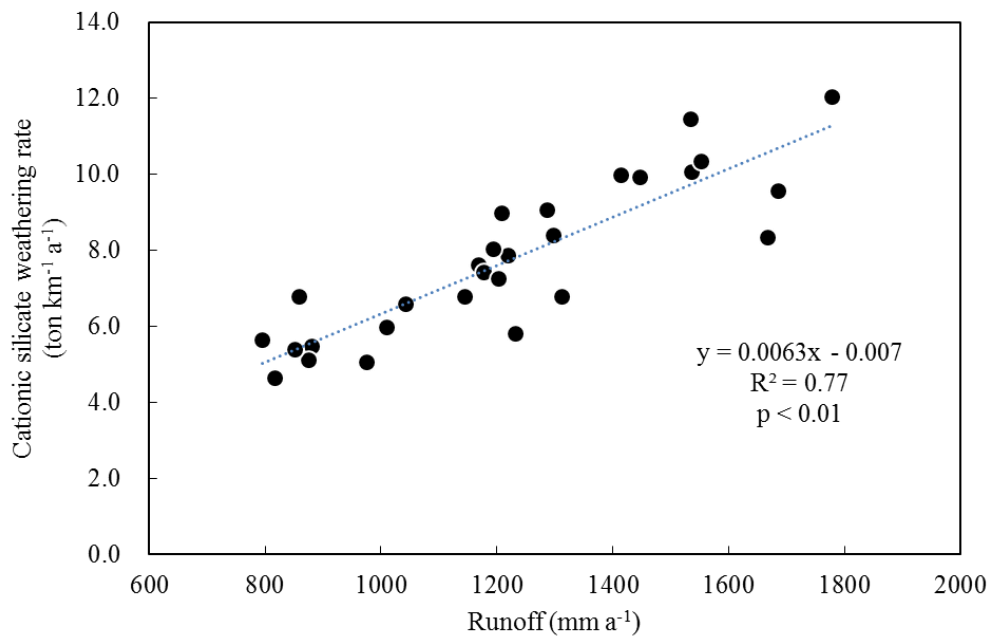


Fig. 5. Plots of the cationic-silicate weathering rate ( $\text{Cat}_{\text{sil}}$ ) vs. runoff for the SECRB, showing that the silicate weathering rates is controlled by the runoff.

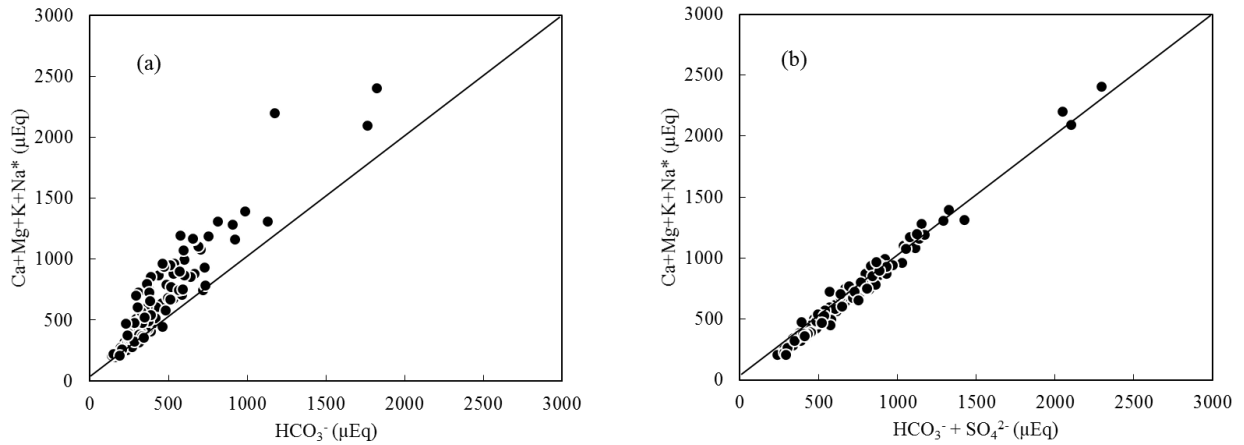


Fig. 6. Plots of total cations derived from carbonate and silicate weathering vs.  $\text{HCO}_3^-$  (a) and  $\text{HCO}_3^- + \text{SO}_4^{2-}$  (b) for river waters in the SECRB.

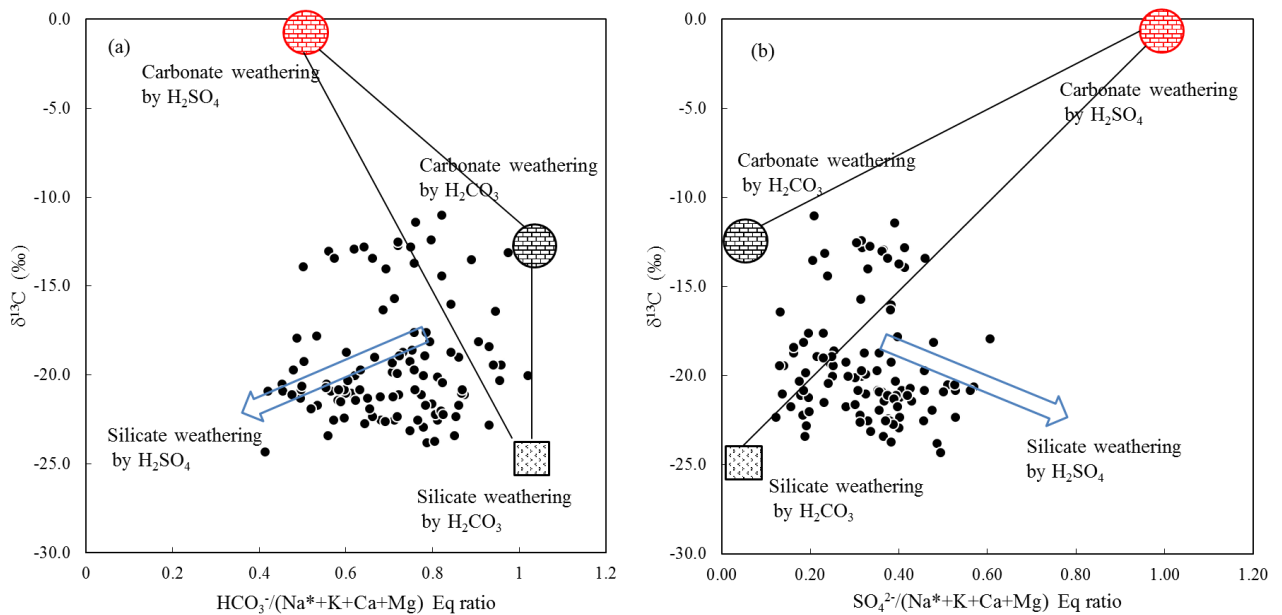


Fig. 7.  $\delta^{13}\text{C}_{\text{DIC}}$  vs.  $\text{HCO}_3^- / (\text{Na}^+ + \text{K}^+ + \text{Ca}^{2+} + \text{Mg}^{2+})$  (a) and  $\text{SO}_4^{2-} / (\text{Na}^+ + \text{K}^+ + \text{Ca}^{2+} + \text{Mg}^{2+})$  Equivalent ratio (b) in river waters draining the SECRB. The plot show that most waters deviate from the three endmember mixing area (carbonate weathering by carbonic acid and sulfuric acid and silicate weathering by carbonic acid), illustrating the effect of sulfuric acid on silicate weathering.